

Supporting Information for the Paper Entitled “Methane Activation and Exchange by Titanium• Carbon Multiple Bonds.”

Jaime A. Flores,[‡] Vincent N. Cavaliere,[‡] Dominik Buck,[‡] Balazs Pinter,[‡] George Chen,[†] Marco G. Crestani,[‡] Mu-Hyun Baik,^{†*} and Daniel J. Mindiola^{†*}

[‡]Department of Chemistry and the Molecular Structure Center, Indiana University, Bloomington, IN 47405.

[†]Division of Chemistry and Chemical Engineering, California Institute of Technology, Pasadena, CA 91125.

Contents

General Considerations	2
Synthesis of (PNP)Ti=CH ^t Bu(CH ₃) (4)	2
Synthesis of isotopologues (4-d ₁ , 4-d ₃ , 4-d ₄)	3
Methane Activation Reactions	4
Reaction of 1 with C ₆ H ₁₂	4
Cyclohexene Detection by Gas Chromatography-Mass Spectrometry	4
Kinetics Experiments	5
Synthesis of (PNP)Ti(μ ₂ -C ^t Bu)(μ ₂ -CH ₃)(AlMe ₂) from (PNP)Ti=CH ^t Bu(CH ₃) and Al(CH ₃) ₃	6
Synthesis of (PNP)Ti(C ^t BuC ^t BuN) from (PNP)Ti=CH ^t Bu(CH ₃) and NC ^t Bu	6
Spectroscopic, Analytical, and Kinetics Data	7
Theoretical Section	28
References	31

Experimental Section

General considerations. Unless otherwise stated, all operations were performed in a M. Braun Lab Master double-dry box under an atmosphere of purified nitrogen. All glassware was either flame or oven-dried overnight and cooled before use. Anhydrous *n*-pentane, diethyl ether, toluene and benzene were purchased from Aldrich as sure-sealed reservoirs (18 L) and dried by passage through a column of activated alumina and then a Q-5 column. Anhydrous cyclohexane was purchased from Aldrich and degassed by the freeze-pump-thaw (FTP) technique. It was then dried over Na metal for 24 hours, passed through a column of alumina and stored over 4 Å molecular sieves. Benzene-*d*₆, cyclohexane-*d*₁₂ and toluene-*d*₈ were purchased from Cambridge Isotope Laboratories (CIL), degassed by FTP and vacuum transferred to an air-tight reservoir containing 4 Å molecular sieves before usage, the following day. Celite, alumina, and 4 Å molecular sieves were activated under vacuum overnight at 200 °C. (PNP)Ti=CH^tBu(OTf) (**3**)¹, (PNP)Ti=CD^tBu(OTf) (**3-d**₁)¹, (PNP)Ti=CH^tBu(CH₂^tBu) (**1**)², Mg(CH₃)₂³ and Mg(CD₃)₂³ were prepared according to literature protocols. Ultra High Purity (99.97%) methane (CH₄) was purchased from Matheson and was used in all sets of reactions. CD₄ was purchased from CIL (Catalog Number: DLM-144-10) and is specified as being 99% deuterated (no specifications are given about the purity of this reagent). Trimethylacetontirie was dried by a two stage vacuum-distillation and degassed by FTP and was dried by passage through a short column of activated alumina immediately prior to use. All other chemicals were used as received. ¹H, ¹³C and ³¹P NMR spectra were recorded on Varian 500, 400 and 300 MHz NMR spectrometers. ¹H and ¹³C NMR spectra are reported with reference to solvent resonances (residual C₆D₅H in C₆D₆, 7.16 ppm and 128.0 ppm respectively). ³¹P NMR chemical shifts are reported with reference to external H₃PO₄ (aqueous solution, 0.0 ppm).

Synthesis of (PNP)Ti=CH^tBu(CH₃) (**4**)

Compound **3** (677 mg, 0.814 mmol) was dissolved in diethyl ether (15 mL) and the solution cooled to -35 °C. Dimethyl magnesium (87 mg, 0.611 mmol) in diethyl ether (3 mL) was then added dropwise and the mixture stirred for 30 min, during which time the color changed from

dark red to yellow-brown. The solvent was removed *in vacuo* and the remaining solid residue was extracted into pentane and filtered through a bed of Celite. The yellow-brown filtrate was concentrated and cooled to –35 °C yielding a pure yellow-orange powder after 3 hours. Yield: 97.5% (444 mg). ^1H NMR (23 °C, 400 MHz, C_6D_6): δ 8.30 (s, 1H, $\text{Ti}=\text{CH}^t\text{Bu}$), 7.22 (m, 1H, C_6H_3), 7.02 (m, 2H, C_6H_3), 6.91 (m, 2H, C_6H_3), 6.84 (m, 1H, C_6H_3), 2.51 (septet, 1H, $J = 7$ Hz, PCHMe_2), 2.38 (overlapped septet, 1H, $J = 7$ Hz, PCHMe_2), 2.34 (overlapped septet, 1H, $J = 7$ Hz, PCHMe_2), 2.16 (s, 3H, $\text{C}_6\text{H}_3\text{CH}_3$), 2.14 (s, 3H, $\text{C}_6\text{H}_3\text{CH}_3$), 1.91 (septet, 1H, $J = 7$ Hz, PCHMe_2), 1.49 (dd, 3H, $\text{PCH}(\text{CH}_3)_2$), 1.41 (dd, 3H, $\text{PCH}(\text{CH}_3)_2$), 1.31 (m, 6H, $\text{PCH}(\text{CH}_3)_2$), 1.23 (s, 9H, $\text{Ti}=\text{CHC}(\text{CH}_3)_3$), 0.97 (m, 9H, $\text{PCH}(\text{CH}_3)_2$), 0.81 (t, $^3J_{\text{H}-\text{P}} = 3$ Hz, 3H, $\text{Ti}-\text{CH}_3$). ^{13}C NMR (23 °C, 100.6 MHz, C_6D_6): δ 160.2 (d, C_6H_3), 156.4 (d, C_6H_3), 133.0 (d, C_6H_3), 132.8 (C_6H_3), 132.7 (C_6H_3), 132.3 (C_6H_3), 129.1 (d, C_6H_3), 125.9 (d, C_6H_3), 120.1 (d, C_6H_3), 119.9 (d, C_6H_3), 119.5 (C_6H_3), 116.2 (d, C_6H_3), 53.4 (br s, $\text{Ti}-\text{CH}_3$), 47.4 ($\text{Ti}=\text{CHCMe}_3$), 33.7 ($\text{Ti}=\text{CHCMe}_3$), 24.9 (d, PCHMe_2), 24.2 (d, PCHMe_2), 21.0 (d, PCHMe_2), 20.7 (d, $\text{C}_6\text{H}_3\text{Me}$), 20.5 (d, $\text{C}_6\text{H}_3\text{Me}$), 20.3 (d, PCHMe_2), 20.3 (d, PCHMe_2), 19.8 (d, PCHMe_2), 19.6 (d, PCHMe_2), 19.1 (d, PCHMe_2), 18.5 (d, PCHMe_2), 18.4 (d, PCHMe_2), 17.5 (d, PCHMe_2), 16.1 (d, PCHMe_2). ^{31}P NMR (23 °C, 162.0 MHz, C_6D_6): δ 32.0 (d, $J_{\text{P}-\text{P}} = 45$ Hz), 21.7 (d, $J_{\text{P}-\text{P}} = 43$ Hz). The neopentylidene carbon resonance could not be located at room temperature because of broadening due to rapid equilibrium between two neopentylidene rotamers. $^{13}\text{C}\{\text{H}\}$ NMR (50 °C, 100.6 MHz, C_6D_6): selected δ 285.4 (br, $\text{Ti}=\text{CH}^t\text{Bu}$). Mp: 150–152 °C (decomp.). HR-MS (CI, positive) Exp: 561.31 [M]⁺, Calc: 561.31; Exp: 562.31 [M+1]⁺, Calc: 562.32; Exp: 560.30 [M-1]⁺, Calc: 560.32.

Synthesis of (PNP) $\text{Ti}=\text{CD}^t\text{Bu}(\text{CH}_3)$ (4-*d*₁), (PNP) $\text{Ti}=\text{CH}^t\text{Bu}(\text{CD}_3)$ (4-*d*₃) and (PNP) $\text{Ti}=\text{CD}^t\text{Bu}(\text{CD}_3)$ (4-*d*₄)

These compounds were synthesized following the same general procedure used for **4**, using a) **3-d**₁ (101.7 mg, 0.123 mmol) and $\text{Mg}(\text{CH}_3)_2$ (5.1 mg, 0.094 mmol); Yield: 58 mg, 82% b) **3** (254.4 mg, 0.306 mmol) and $\text{Mg}(\text{CD}_3)_2$ (19.0 mg, 0.315 mmol); Yield: 177 mg 87% and c) **3-d**₁ (157.8 mg, 0.189 mmol) and $\text{Mg}(\text{CD}_3)_2$ (11.1 mg, 0.182 mmol) Yield: (158 mg, 83.9%) respectively.

Methane Activation Reactions

In a typical reaction, compound **1** (0.010 g, 0.016 mmol) was dissolved in cyclohexane-*d*₁₂ (0.4 mL) and transferred into a single-crystal sapphire NMR tube equipped with a high-pressure manifold, a gas purifier, and protecting polycarbonate casing for the NMR tube.⁴ Next, the NMR tube was pressurized with methane to 1150 psi and carefully tilted to facilitate dissolution of methane (the tube could not be inverted to avoid contamination of the piston). This procedure was repeated to ensure the correct pressure in the NMR tube. Integration of the methane signal (0.17 ppm) in the ¹H NMR spectrum revealed approximately 62 equivalents of methane in solution. The reaction was subsequently monitored by ³¹P NMR over 11 hours at 31 °C. (PNP)Ti=CH^tBu(CH₃) was obtained in 84% spectroscopic yield. Measurements at 310 and 725 psi were conducted analogously. (For a detailed description of the high-pressure reactor used, see reference ⁴)

The same reaction was performed with CD₄ (260 psi, 31 °C) using the same set-up to form the isotopologue, (PNP)Ti=CD^tBu(CD₃), after 12 hours.

Reaction of **1** with C₆H₁₂

In a J-Young NMR tube **1** (43.5 mg, 0.0704 mmol) was dissolved in C₆H₁₂. The NMR tube was placed in a Varian i400 NMR spectrometer with the probe set at 31 °C. The reaction was monitored by ³¹P NMR for 24 h, during which time the starting material decomposed to myriad products.

Cyclohexene Detection by Gas Chromatography-Mass Spectrometry (GC-MS)

Following the reaction of **1** with C₆H₁₂, 10 uL of vapor from the headspace of the J-Young NMR tube was injected into a Trace GC (Thermo Electron Corporation, Waltham, MA) equipped with a 0.25mm x 60 m Agilent DB-VRX GC column (1.4 um film thickness, Agilent Technologies, S4

Santa Clara ,CA). A 40:1 split ration was employed and 1.0 mL/min of He gas was the mobile phase for the separation. The temperature program was: hold at 40 °C for 1 minute, ramp 5 °C/min to 150 °C, ramp 15 °C/min to 200 °C with a total run time of 26 minutes. The column was directed into the electron ionization source of a MAT-95 magnetic sector mass spectrometer scanning from 35-200 m/z at 1.5 sec/decade. Cyclohexane eluted at 13.84 minutes; the 67 Da and 54 Da fragments of cyclohexene wes observed at 14.57 minutes.

Kinetics Experiments

For the **1 → 4** or **4-d₄** conversion and control experiment in C₆H₁₂, reactions were performed according to the prescribed procedures on pg. S2 and S3 respectively. To determine the rate constant, *k*, for these reactions, the peaks assigned to compound **1** (28.4, 20.4 ppm) in the ³¹P NMR spectrum were integrated for each spectrum acquired during the run (approx. 166 seconds between each spectrum) and normalized with respect to an internal reference of H₃PO₄ (0.00 ppm) in a sealed capillary. The reaction was allowed to proceed to ~88% conversion. The integrations of both doublets in the ³¹P NMR spectrum were summed (INT_t) and pseudo-first-order plots were constructed by charting ln(INT_t/INT₀) vs. time (Figures S24 and S25).

For the **4 → 2-d₆** conversion, compound **4** (25 mg) was dissolved in C₆D₆ (1 mL) in a sealed J-Young NMR tube and the solution was heated to a) 60, b) 70, c) 80 and d) 90 °C in a calibrated oil bath. Conversion to compound **2-d₆** was monitored by ³¹P NMR spectroscopy. No byproducts were observed. Temperature dependent experiments were performed in triplicate for each temperature run. The rate constants, *k*, were determined in the same manner as above (Figures S26 and S27). **Kinetic Isotopic Effects (KIE)** were determined in an analogous manner to this, using the appropriate isotopologue **4-d₁**, **4-d₃** or **4-d₄**.

Synthesis of (PNP)Ti(μ_2 -C^tBu)(μ_2 -CH₃)(AlMe₂) from 4 and Al(CH₃)₃

In a J-Young NMR tube, **4** (30 mg, 0.053 mmol) was dissolved in C₆D₆ (1 mL) and the solution was frozen at -35 °C. Trimethylaluminum (3 drops 1.0 M in heptanes, excess) was then added and the solution was allowed to warm up to room temperature. This was then stirred for 1 hour, during which time the color changed from yellow to deep red. At this time, the solvent was removed *in vacuo* and the residue was extracted into pentane. The solution was cooled to -35 °C and a deep red solid was obtained after ~12 hours. Conversion into (PNP)Ti=C^tBuAl(CH₃)₂(μ -CH₃) was confirmed by ³¹P and ¹H NMR spectroscopy and comparing with an authentic sample of (PNP)Ti(μ_2 -C^tBu)(μ_2 -CH₃)(AlMe₂).⁵ Yield: 78.9% (26 mg).

Synthesis of (PNP)Ti(C^tBuC^tBuN) from 4 and NC^tBu

4 (37 mg, 0.066 mmol) was dissolved in trimethylacetonitrile (1 mL) and the resulting yellow solution was stirred for 8 days at room temperature. An orange precipitate was formed after this time. Standard work-up and overnight recrystallization from cold n-pentane yielded the pure product; the identity of which was confirmed by comparison with the reported ³¹P and ¹H NMR spectra of this compound.⁶ Yield: 72.0% (30 mg).

Selected Spectroscopic, and Kinetics Data

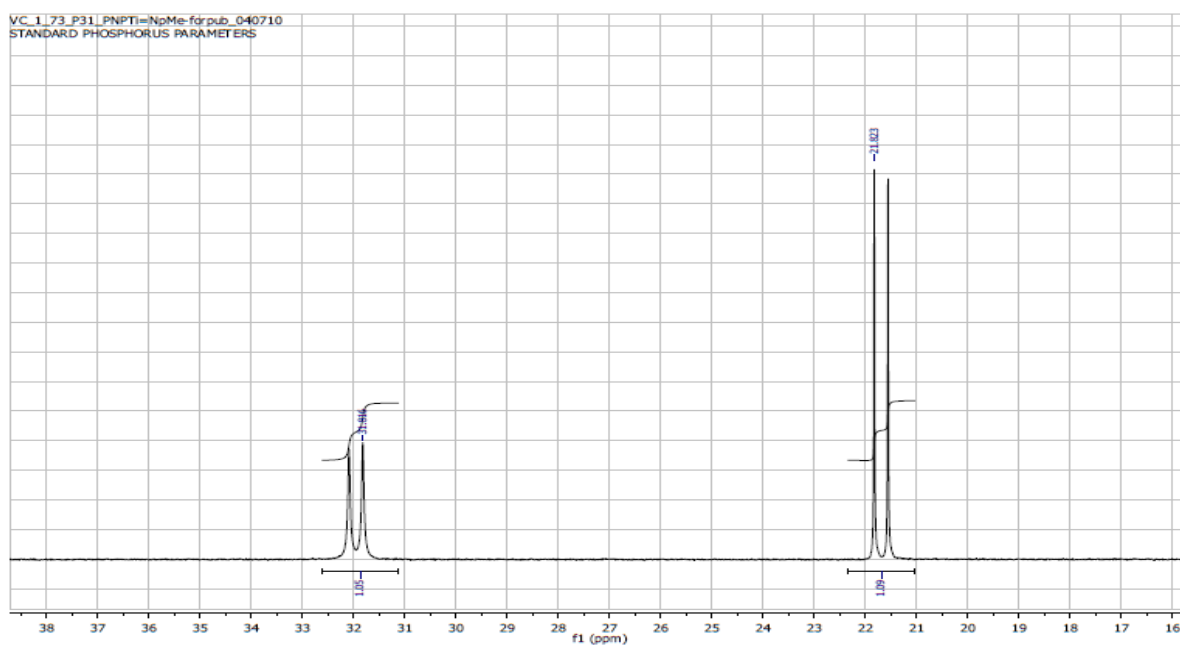


Figure S1. $^{31}\text{P}\{\text{H}\}$ NMR spectrum of **4** in C_6D_6 at 23 °C.

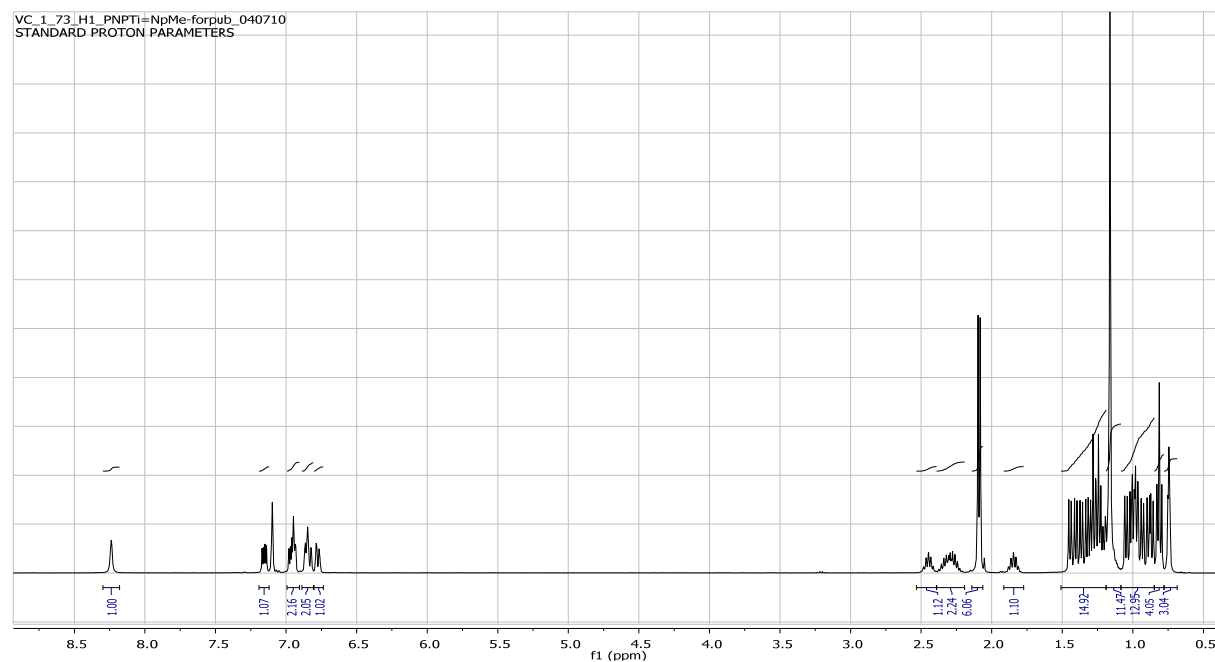


Figure S2. ^1H NMR spectrum of **4** in C_6D_6 at 23 °C.

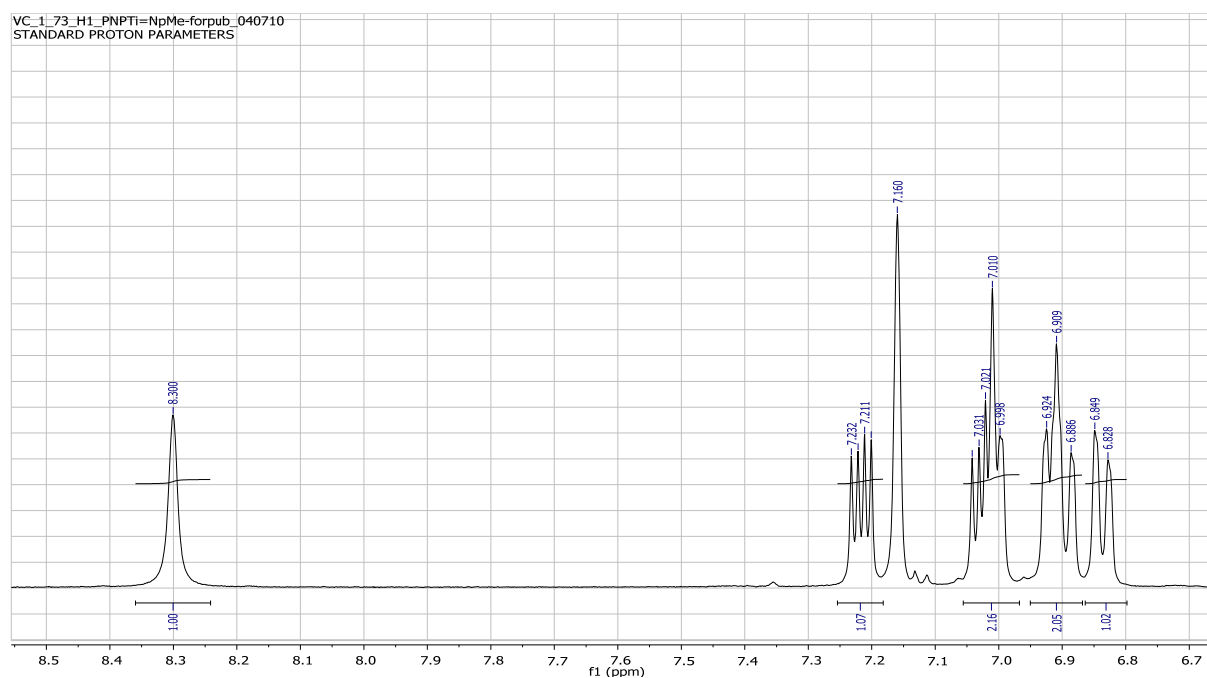


Figure S3. Expanded ¹H NMR spectrum of **4** in C₆D₆ at 23 °C.

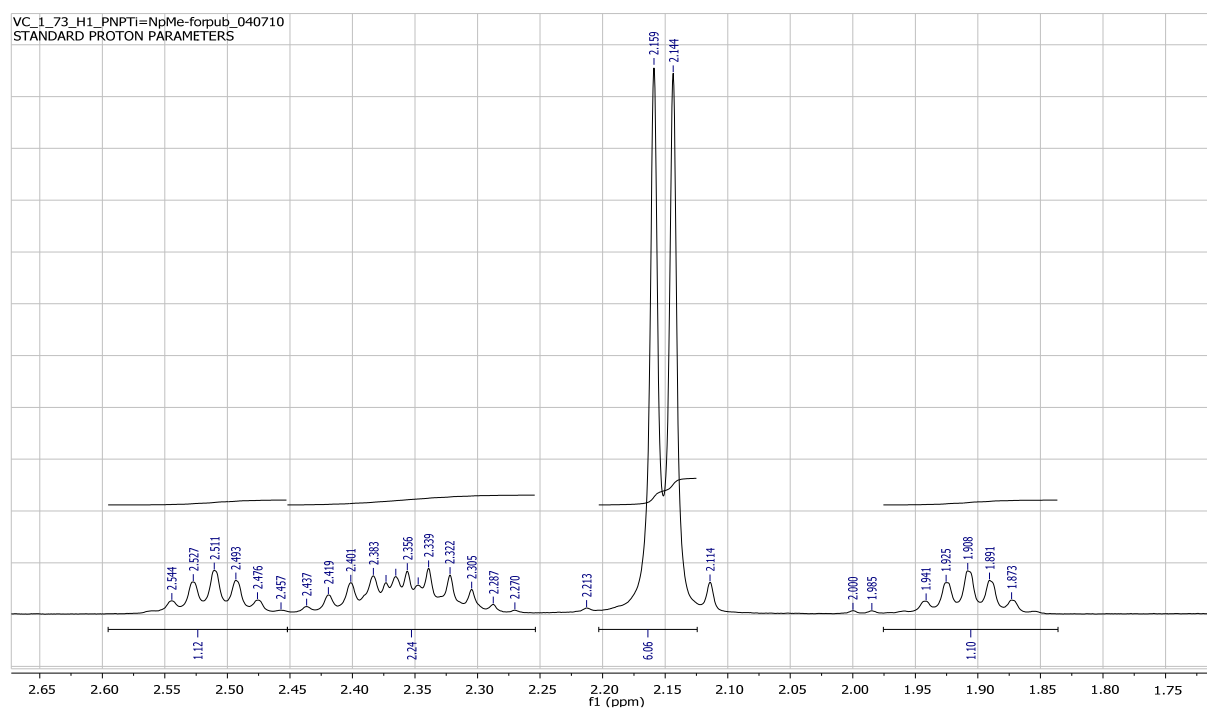


Figure S4. Expanded ¹H NMR spectrum of **4** in C₆D₆ at 23 °C.

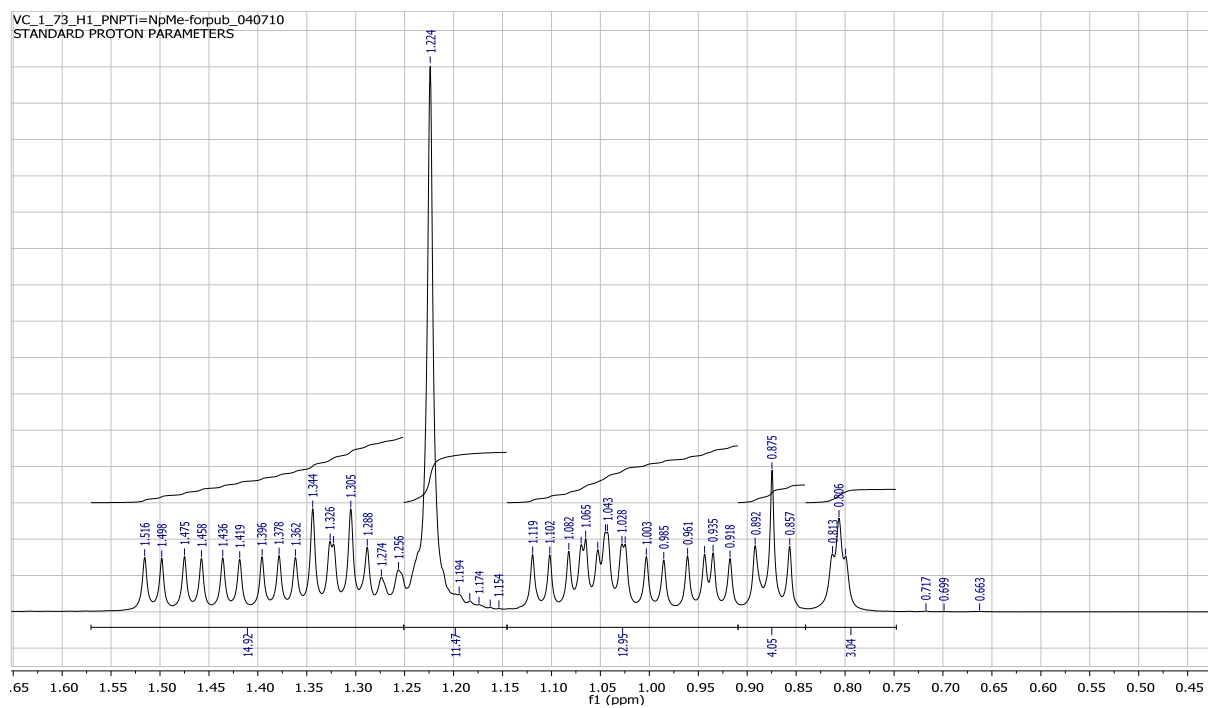


Figure S5. Expanded ¹H NMR spectrum of **4** in C₆D₆ at 23 °C.

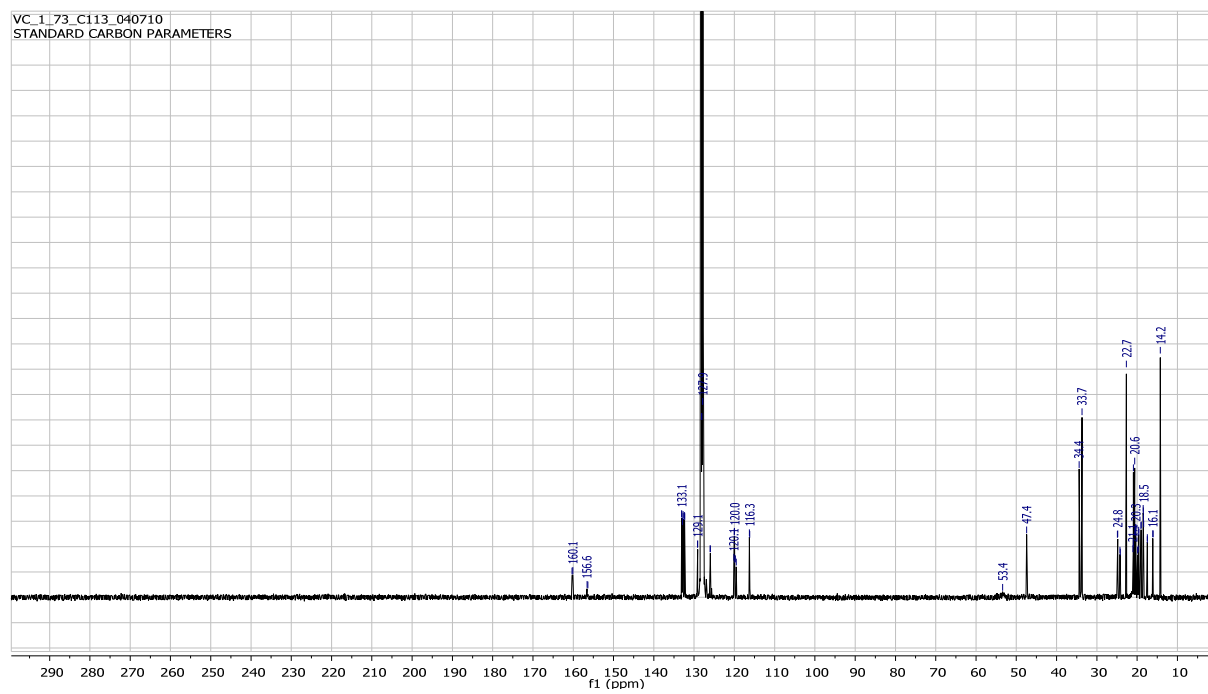


Figure S6. ¹³C{¹H} NMR spectrum of **4** in C₆D₆ at 23 °C.

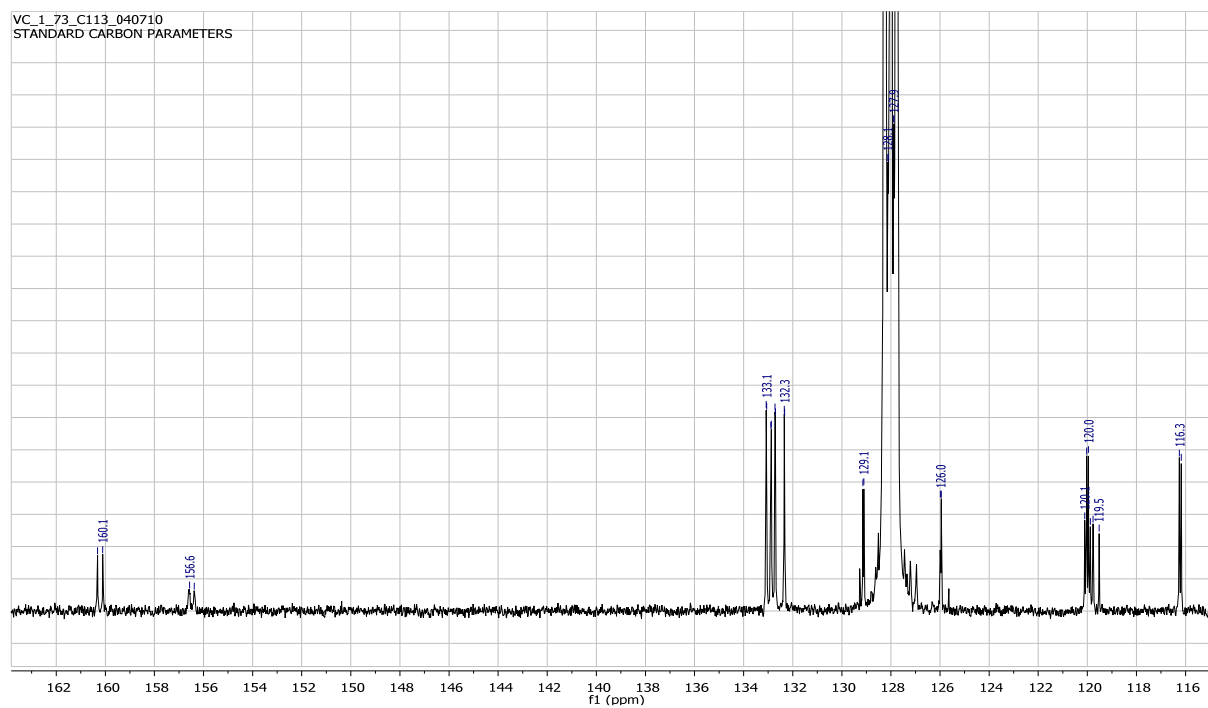


Figure S7. $^{13}\text{C}\{^1\text{H}\}$ NMR spectrum of **4** in C_6D_6 at $23\text{ }^\circ\text{C}$.

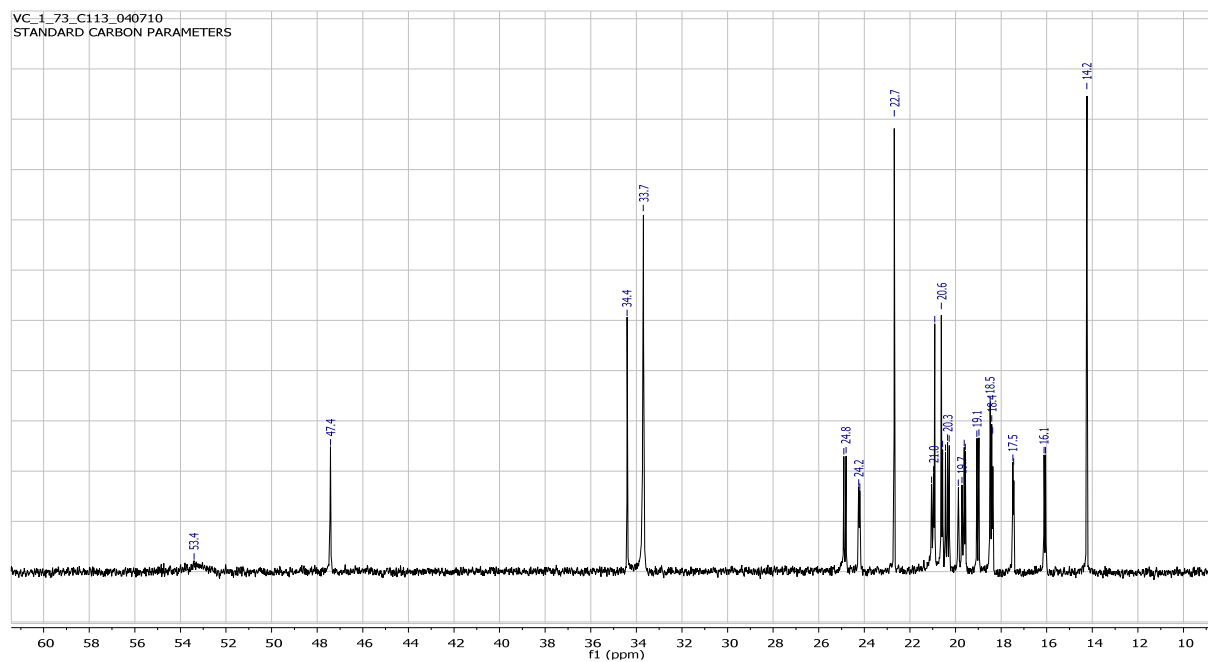


Figure S8. $^{13}\text{C}\{^1\text{H}\}$ NMR spectrum of **4** in C_6D_6 at $23\text{ }^\circ\text{C}$.

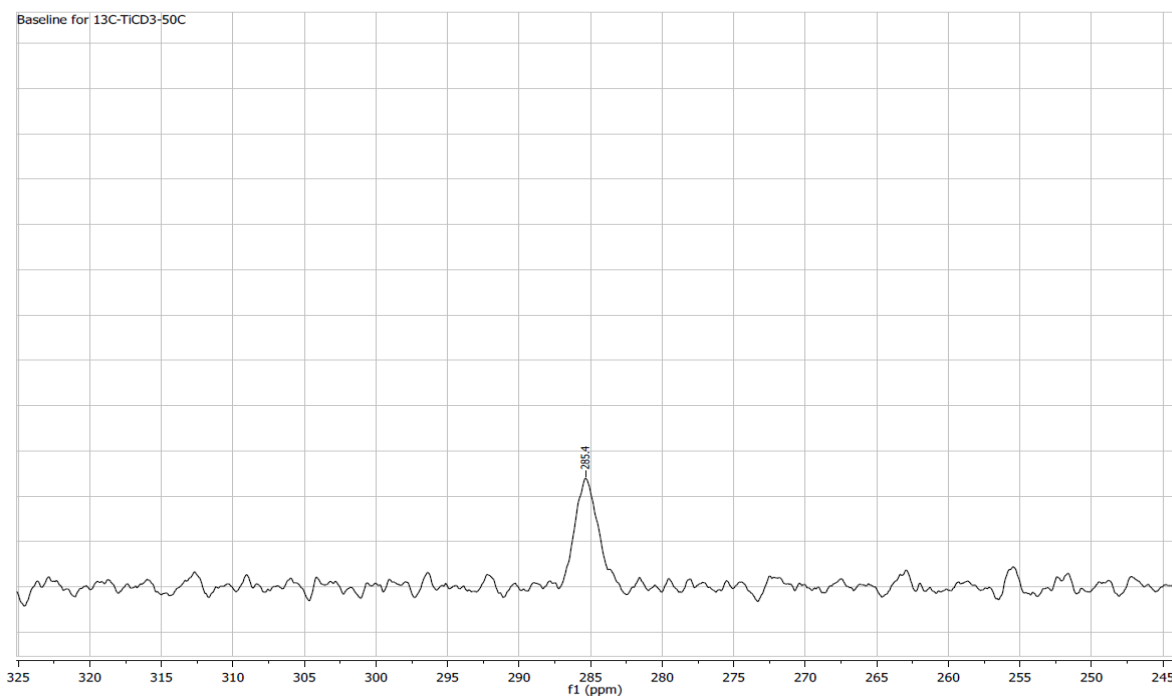


Figure S9. $^{13}\text{C}\{^1\text{H}\}$ NMR signal of **4** in C_6D_6 at $50\text{ }^\circ\text{C}$.

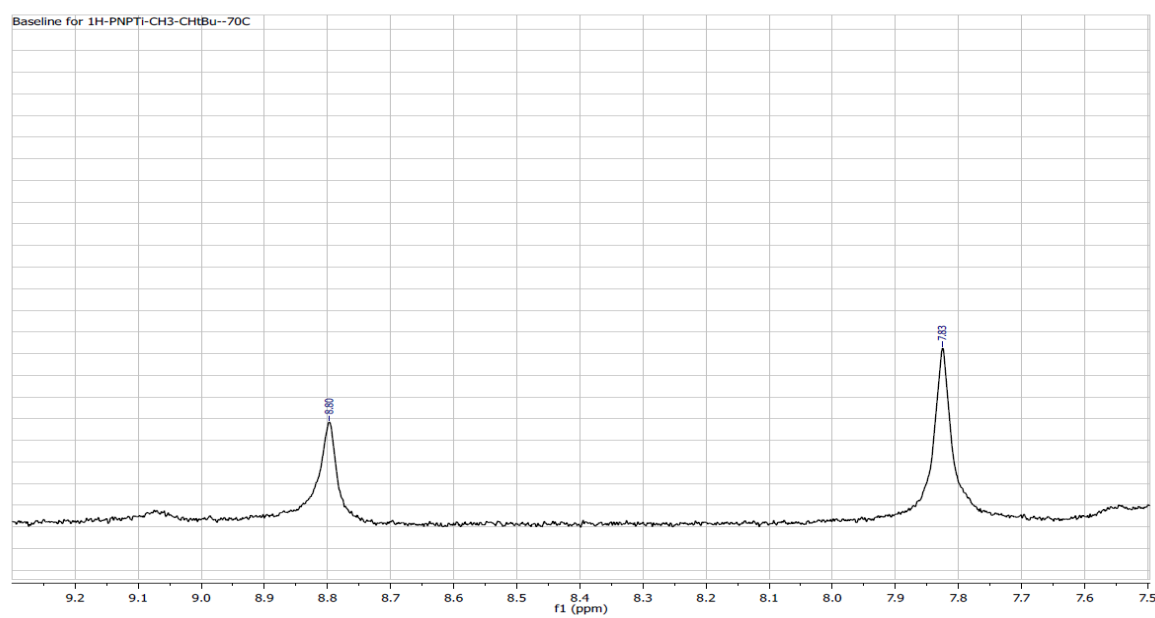
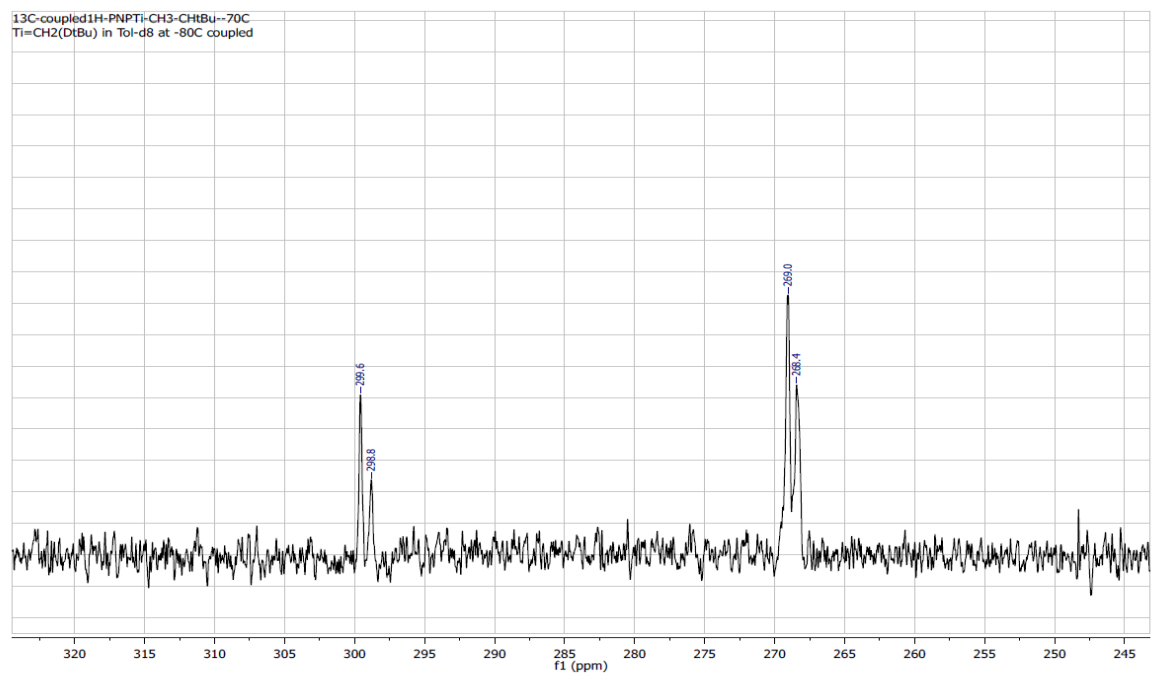


Figure S10. ^1H NMR signals of **4-anti** and **4-syn** in toluene- d_8 at $-70\text{ }^\circ\text{C}$.



F

figure S11. Expanded ¹³C NMR spectrum showing signals of **4-anti** and **4-syn** in toluene-*d*₈ at -70 °C.

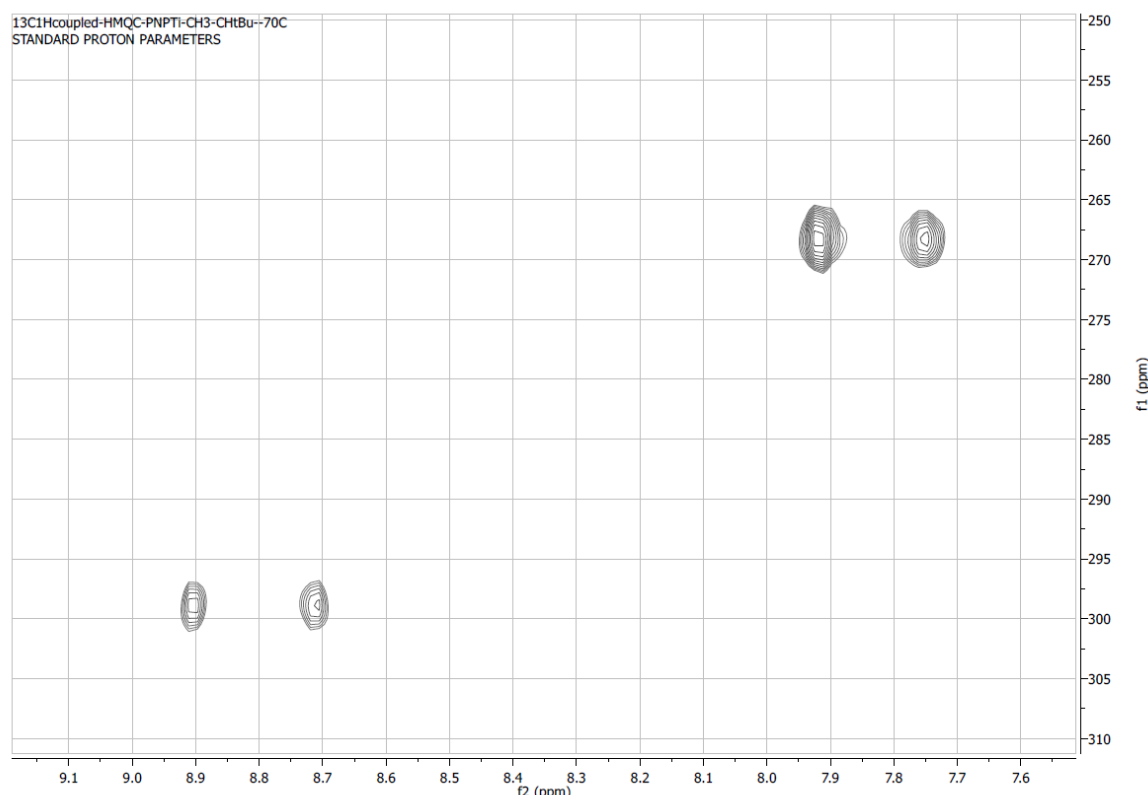


Figure S12. Expanded ^{13}C - ^1H HMQC NMR spectrum showing resonances of **4-anti** and **4-syn** in toluene- d_8 at $-70\text{ }^\circ\text{C}$.

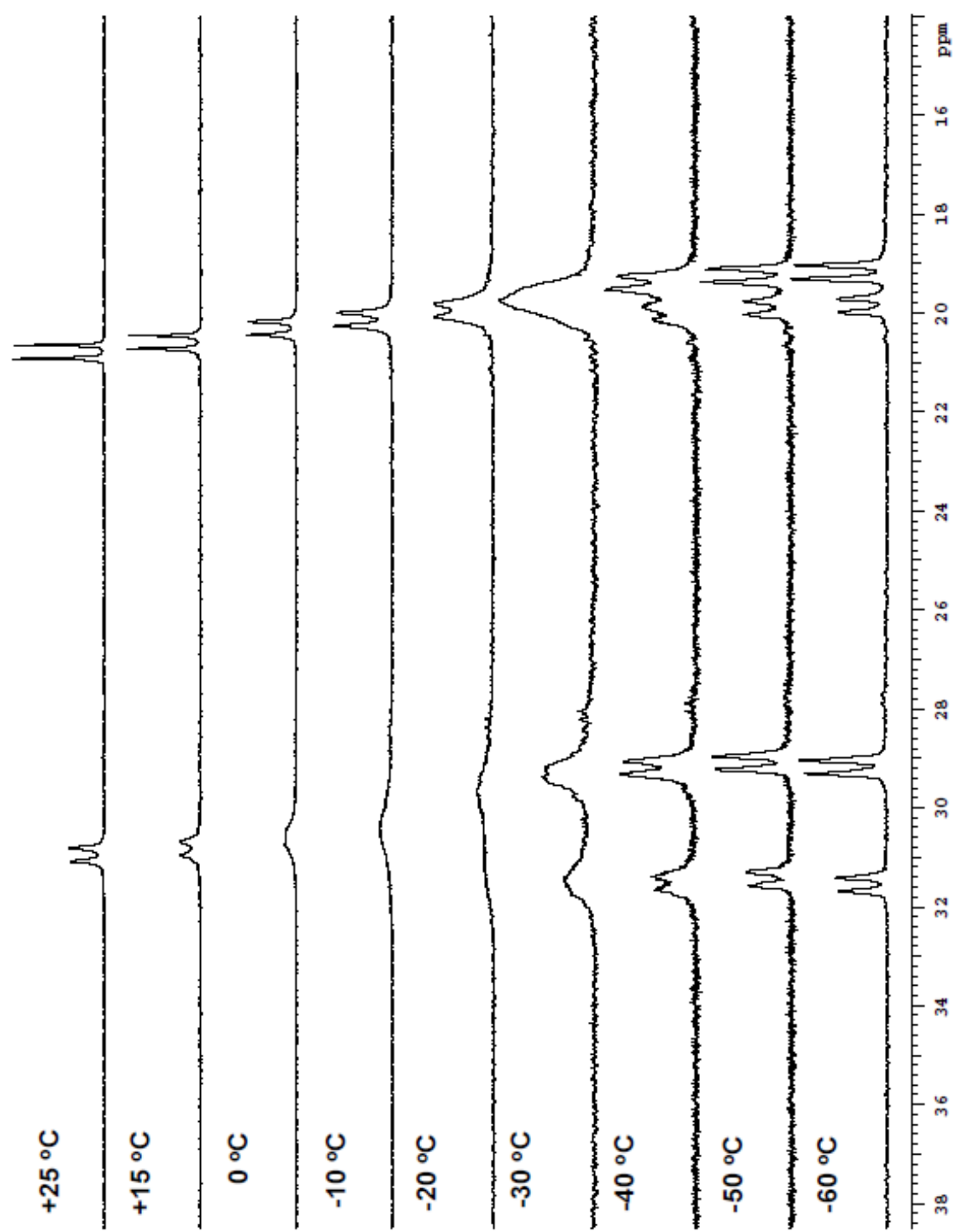


Figure S13. Variable temperature- $^{31}\text{P}\{\text{H}\}$ NMR spectra of **4** in toluene- d_8 , from -60 to 25 °C.

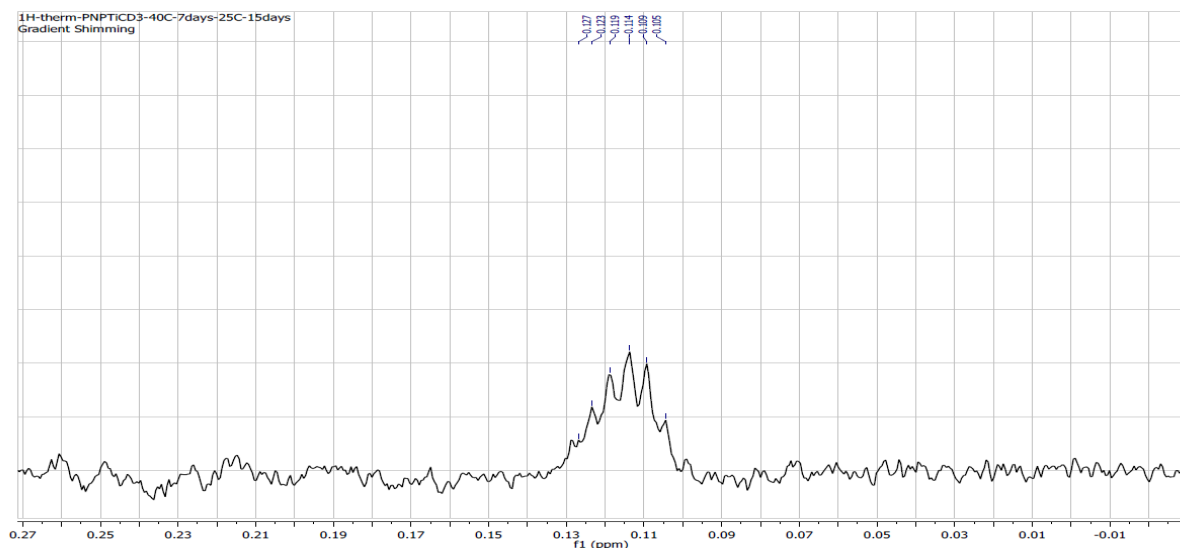


Figure S14. Expanded ¹H NMR spectrum of CD₃H from the thermolysis of (PNP)Ti=CH^tBu(CD₃) (**4-d**₃) in C₆D₆ at 80 °C.

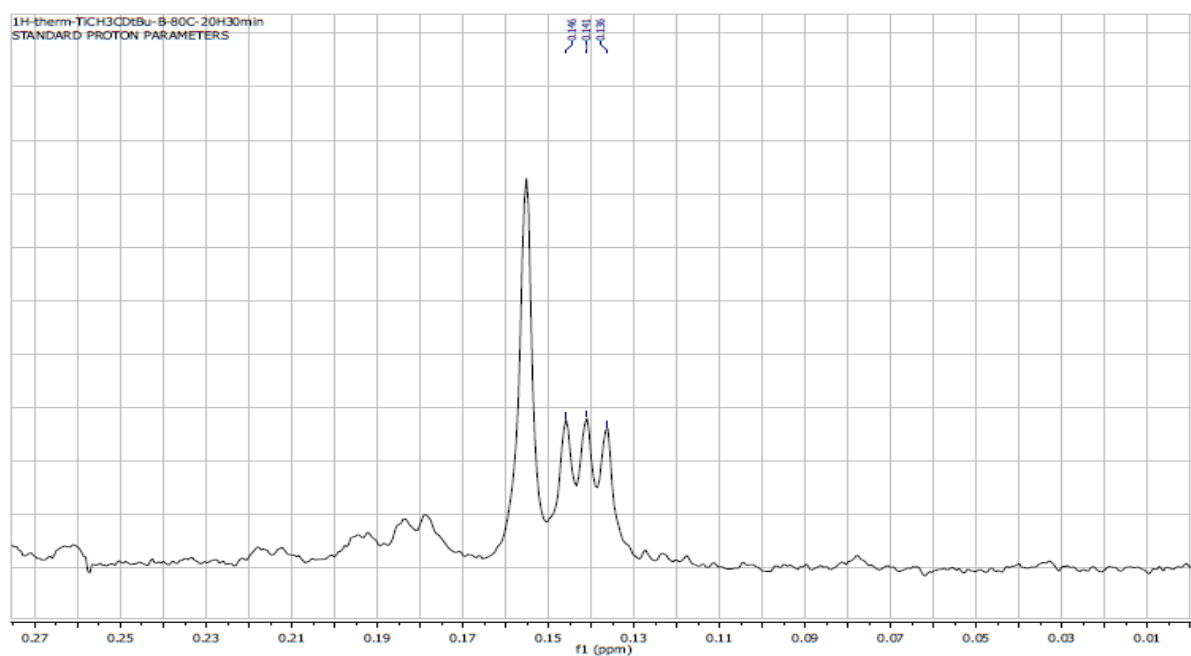


Figure S15. Expanded ¹H NMR spectrum of CDH₃ from the thermolysis of (PNP)Ti=CD^tBu(CH₃) (**4-d**₁) in C₆D₆ at 80 °C.

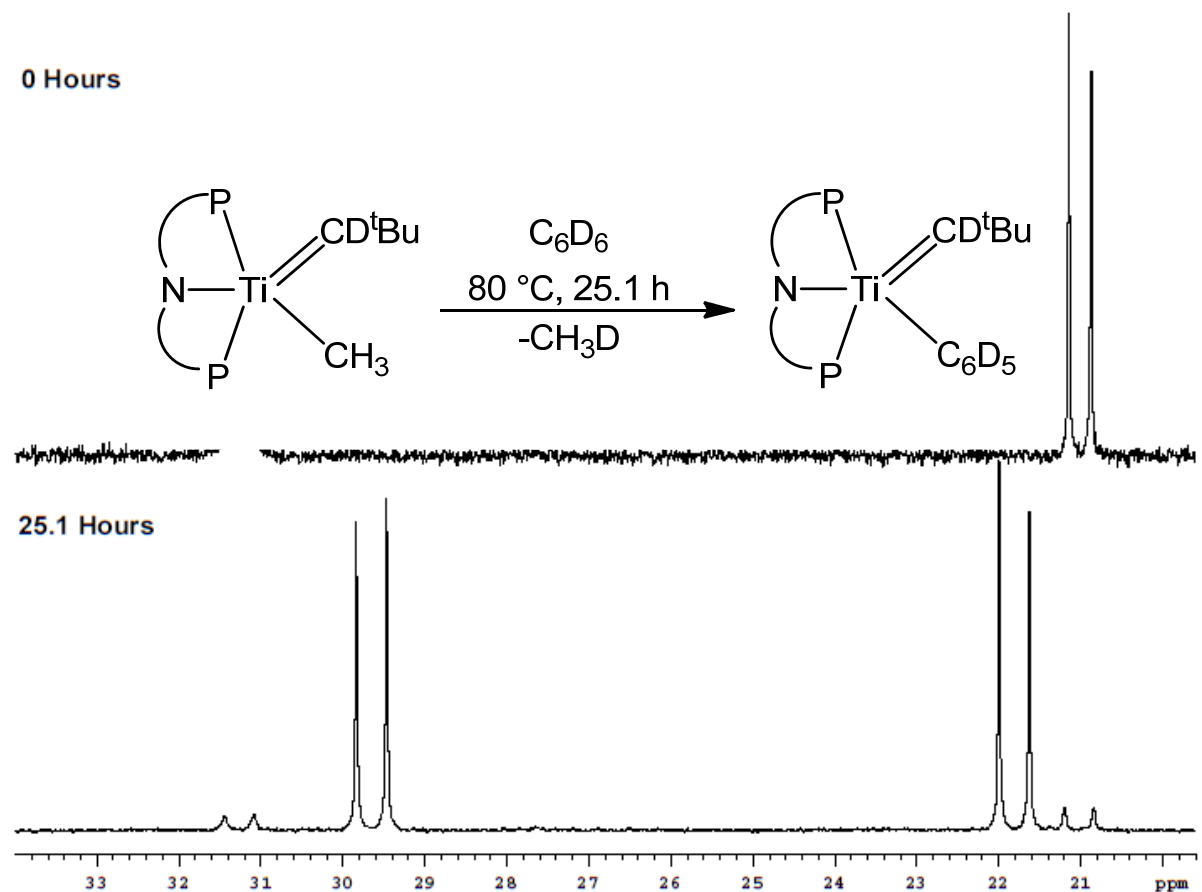


Figure S16. $^{31}\text{P}\{\text{H}\}$ NMR spectra of the thermolysis of 4-*d*₁ in C₆D₆ at 80 °C: stacked spectra at *t* = 0 and *t* = 25.1 h

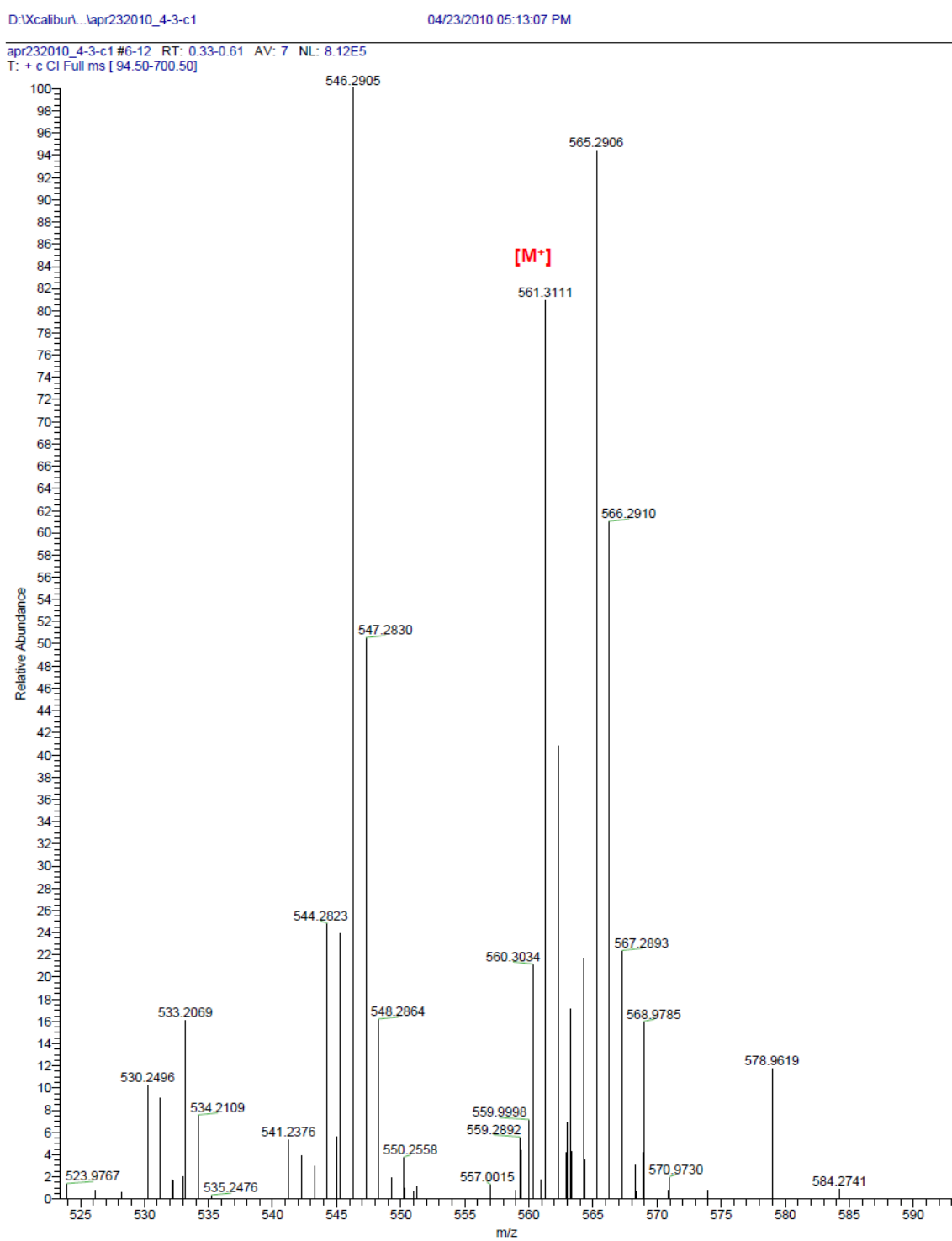


Figure S17. High-resolution chemical-ionization mass-spectrum (HR-CI-MS) of **4**.

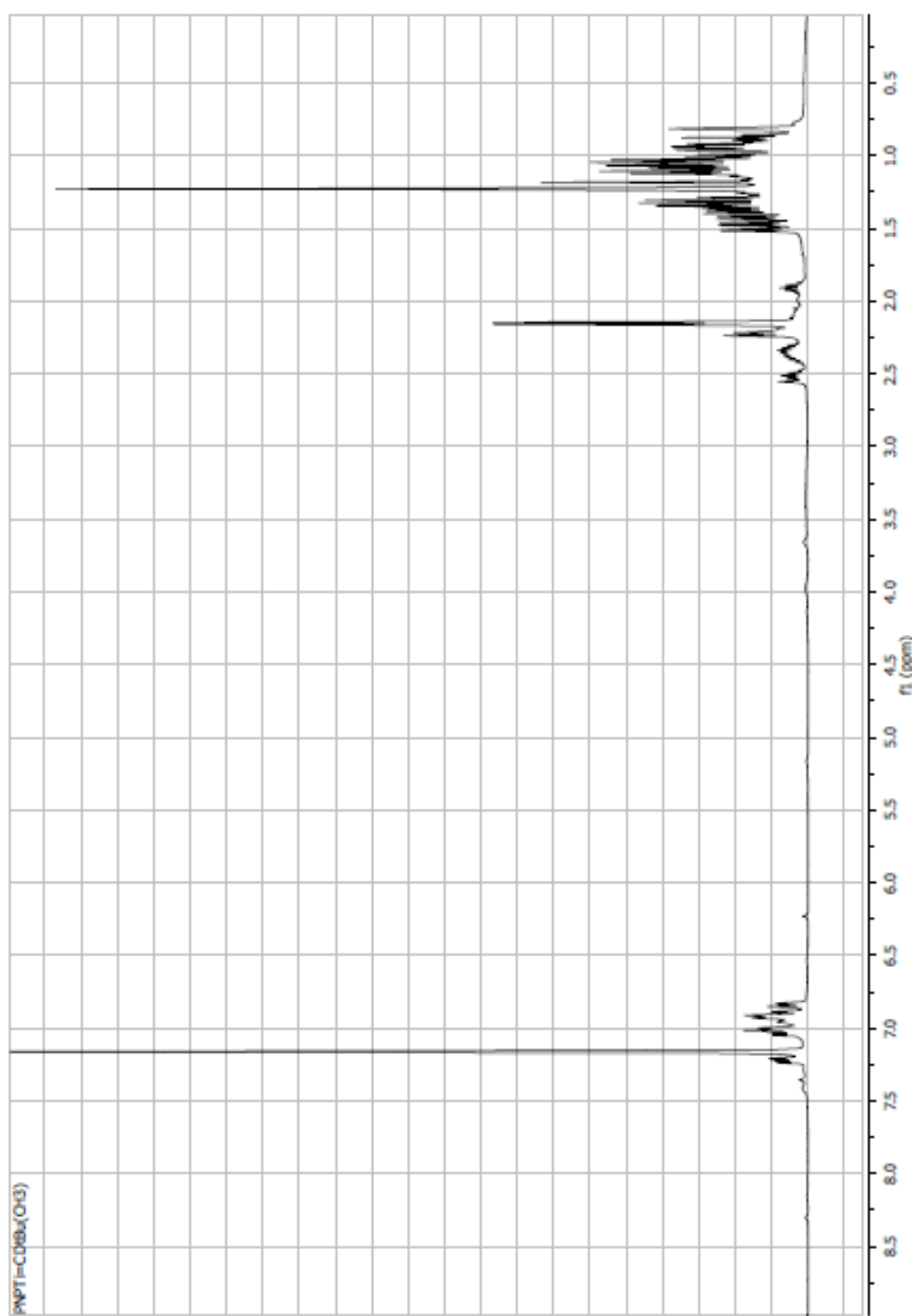


Figure S18. ¹H NMR spectrum of **4-d₁** in C_6D_6 at 23 °C.

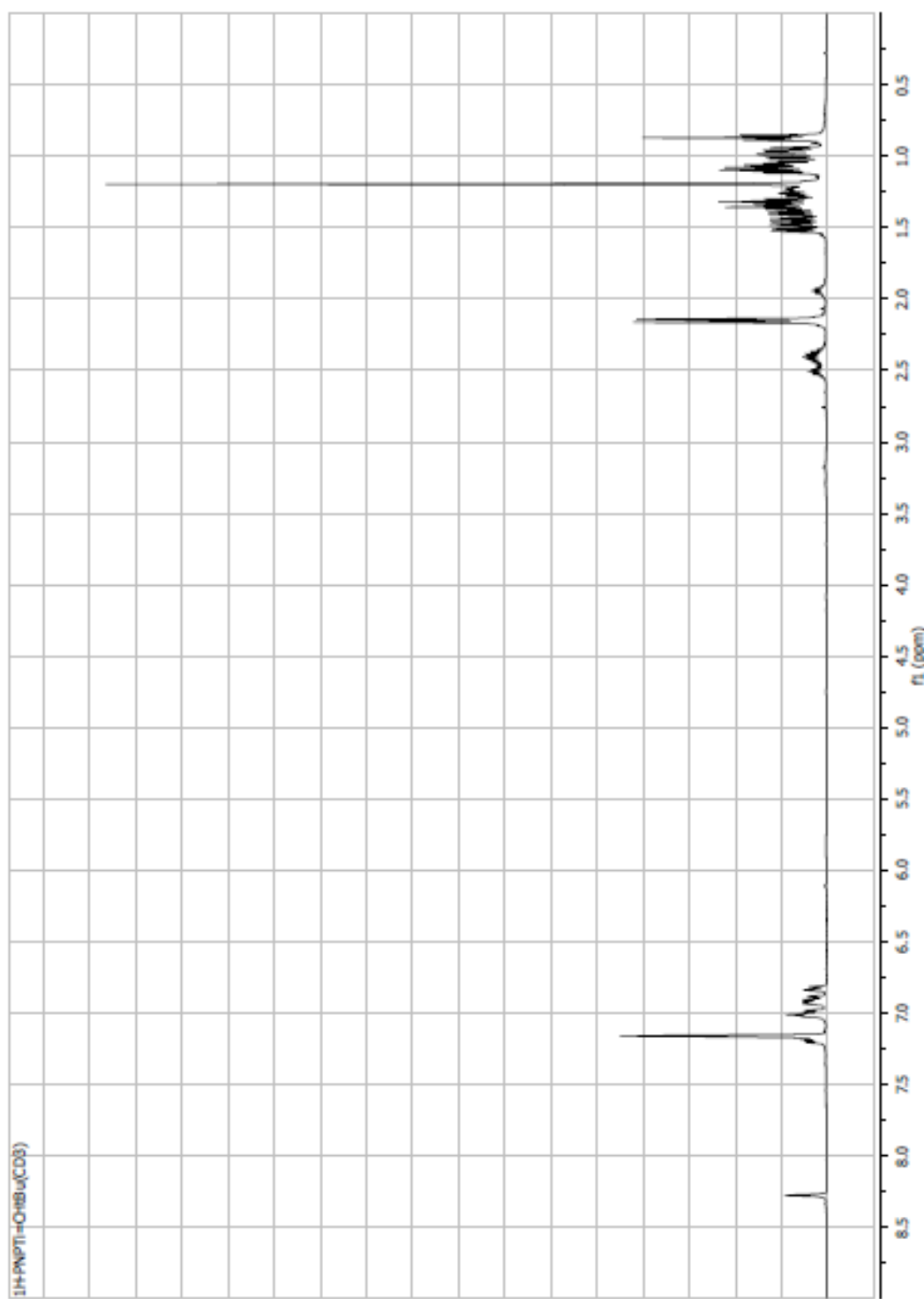


Figure S19. ¹H NMR spectrum of **4-d₃** in C_6D_6 at 23 °C.

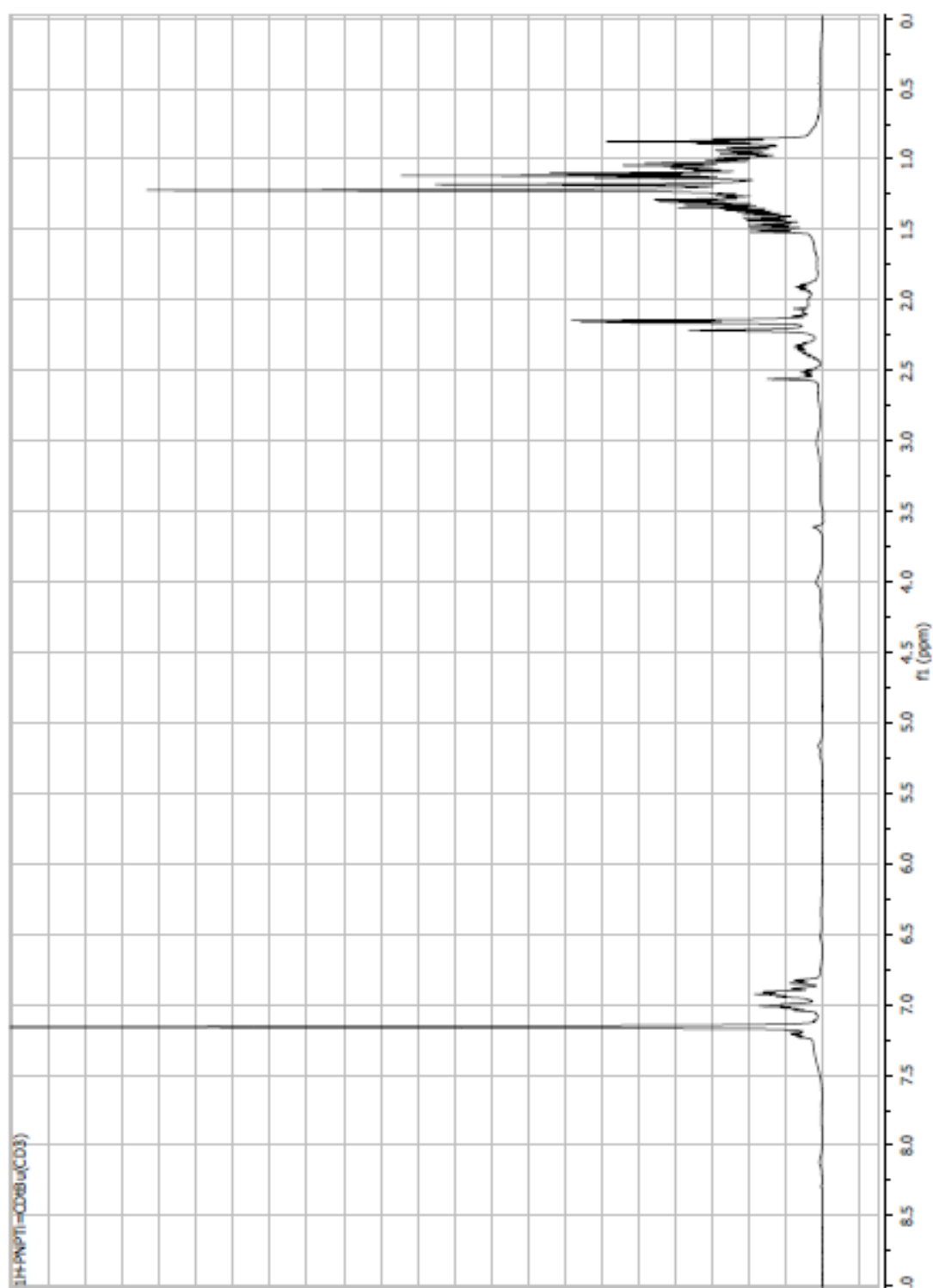


Figure S20. ¹H NMR spectrum of **4-d₄** in C_6D_6 at 23 °C.

S20

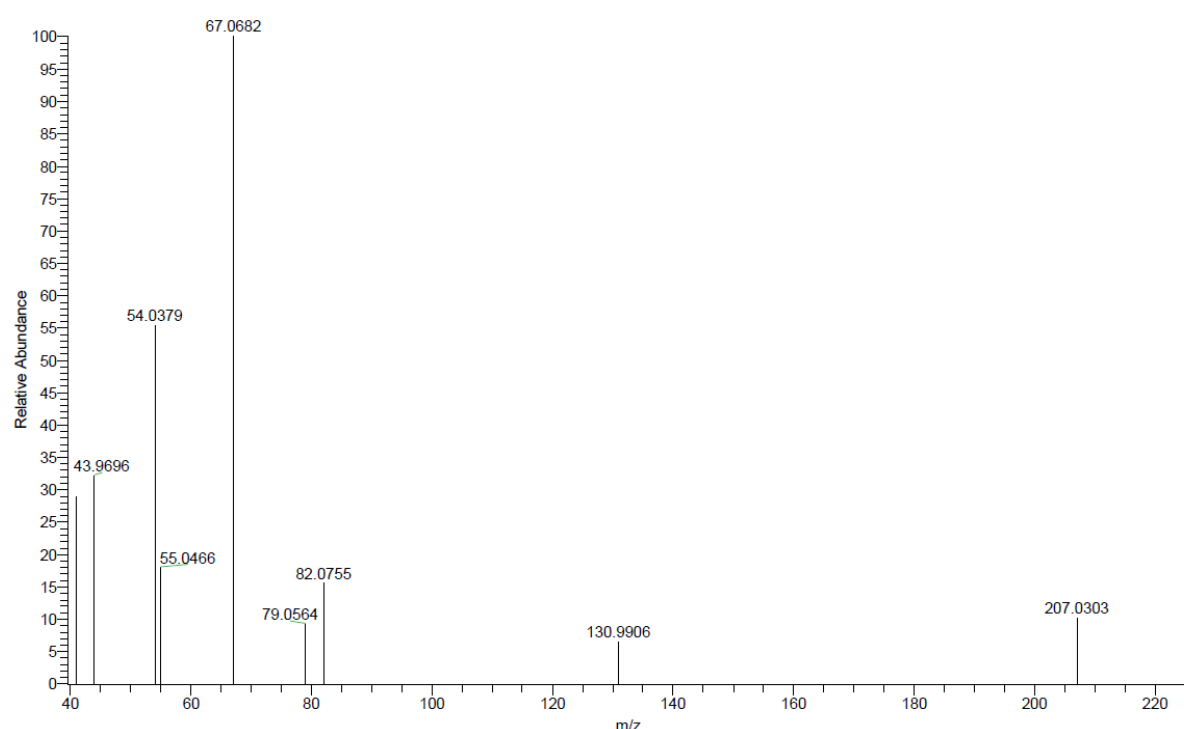


Figure S21. High-resolution electron-ionization mass-spectrum (HR-EI-MS) of cyclohexene obtained from the headspace of the reaction of **1** with C₆H₁₂.

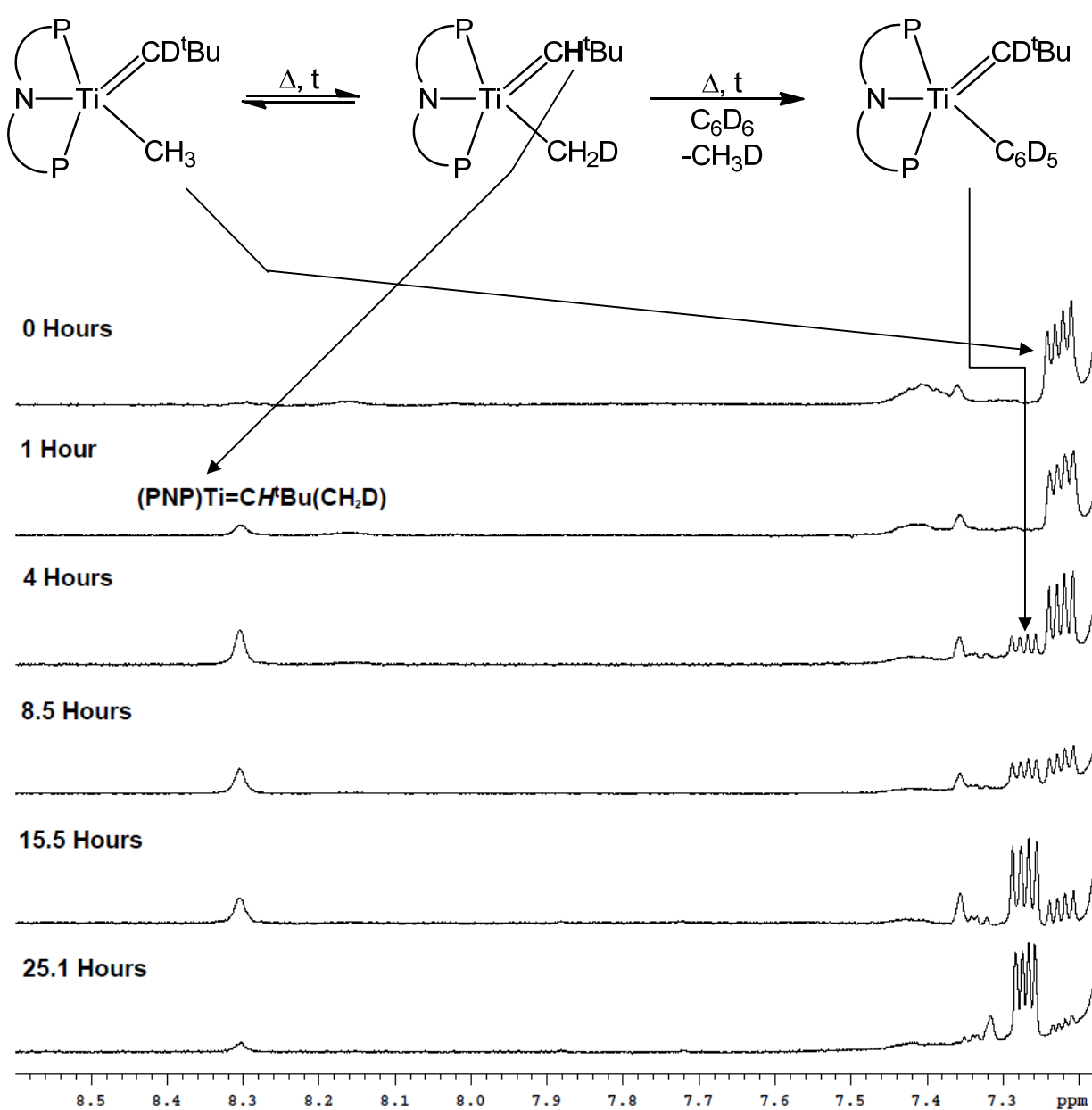


Figure S22. Low-field expansions of stacked ¹H NMR spectra obtained from thermolysis of **4-d₁** in C₆D₆ at 80 °C. Scrambling of H into the Ti=CH^tBu position is observed at 8.3 ppm within 1 hour. For the isotopologues, **4-d₁** and **3-d₆**, peaks near 7.3 ppm correspond to ¹H NMR signals from the PNP-backbone.

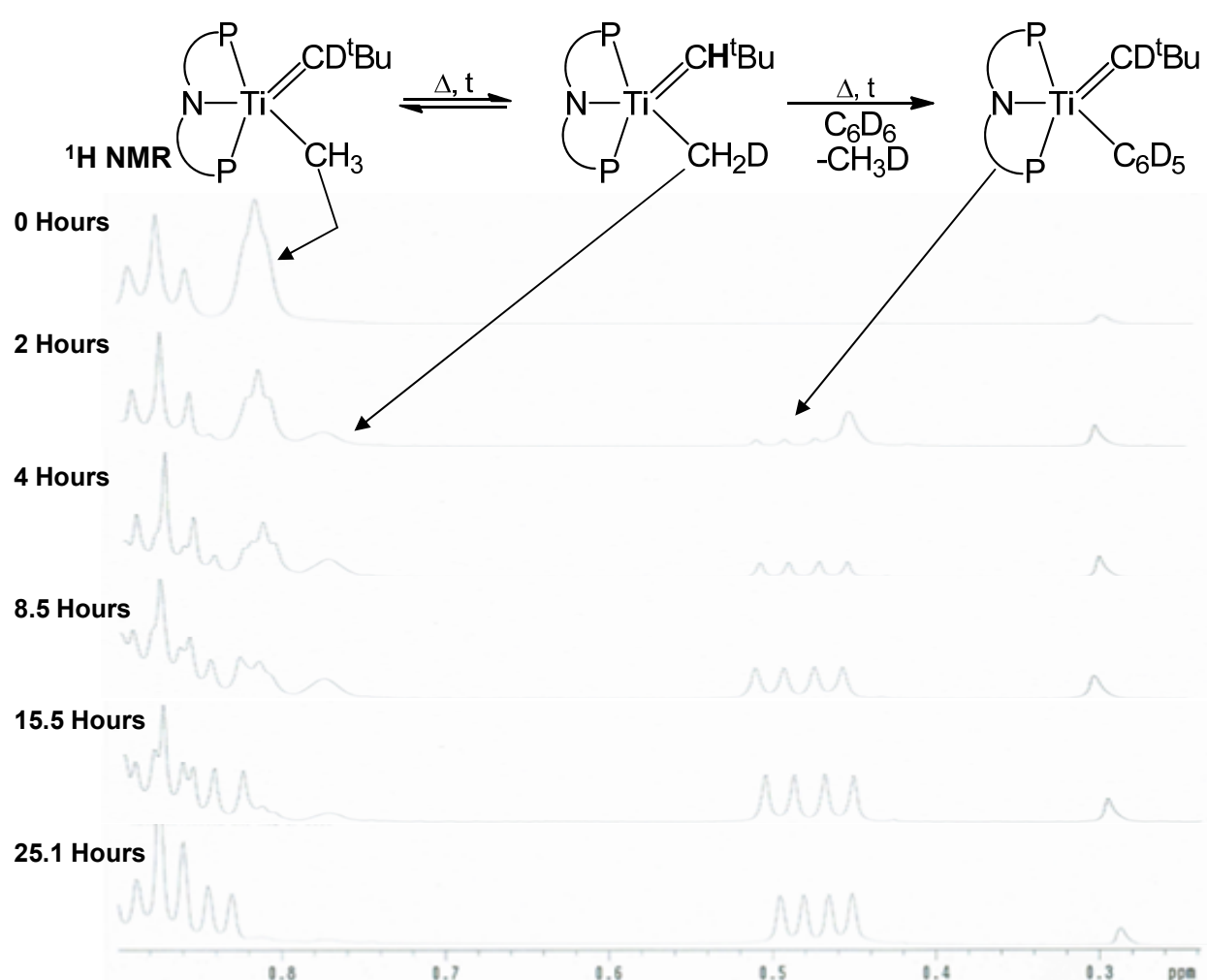


Figure S23. High-field expansions of stacked ¹H NMR spectra for the thermolysis of **4-d₁** in C₆D₆ at 80 °C. Scrambling of D into the Ti-CDH₂ position is observed at ~0.8 ppm after several hours. The signal assigned for **3-d₆** corresponds to one of the four inequivalent isopropyl-methyls on the PNP ligand.

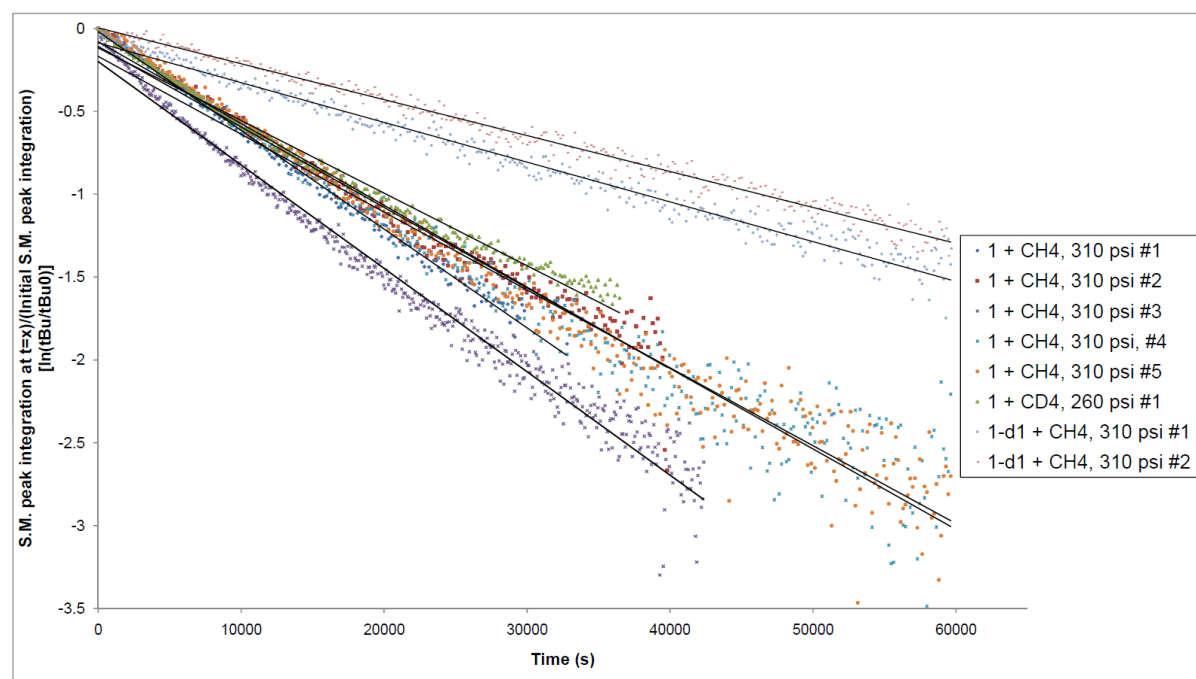


Figure S24. First-order plot showing the comparative rates for reactions involving **1** + CH₄ (310 psi) or CD₄ (260 psi) or **1-d1** + CH₄ (310 psi)

Table S1. Summarized rates for all methane activation experiments in **Figure S24**

Compound	Reagent	Pressure (psi)	k ($\times 10^{-5} \text{ s}^{-1}$)
1	CH ₄	310	5.963
1	CH ₄	310	4.941
1	CH ₄	310	6.241
1	CH ₄	310	4.700
1	CH ₄	310	4.858
1	CH ₄	725	7.181
1	CH ₄	1150	7.856

1	CD ₄	260	4.383
1-d₁	CH ₄	310	2.169
1-d₁	CH ₄	310	2.398

Table S2. KIE ($k_{\text{H}}/k_{\text{D}}$) for CH₄ vs. CD₄ and **1** vs. **1-d₁**

CH ₄ vs. CD ₄	1.2(1)
1 vs. 1-d₁	2.3

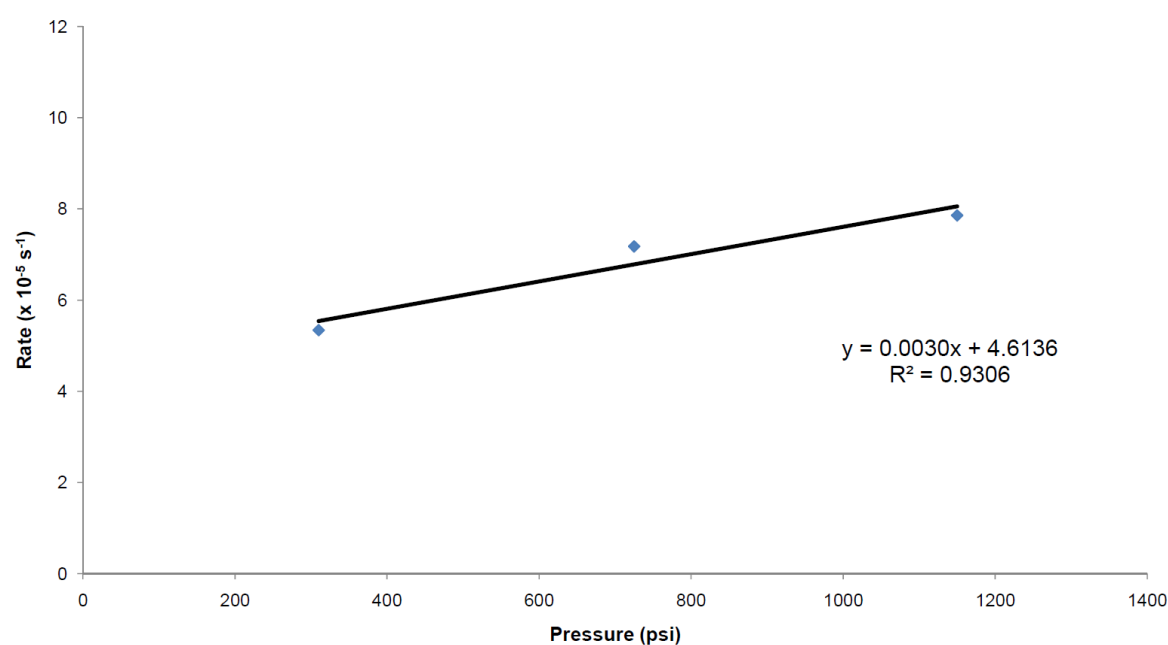


Figure S25. Plot of average rate versus pressure (310, 725, 1150 psi) for conversion of **1** to **4** in C₆H₁₂

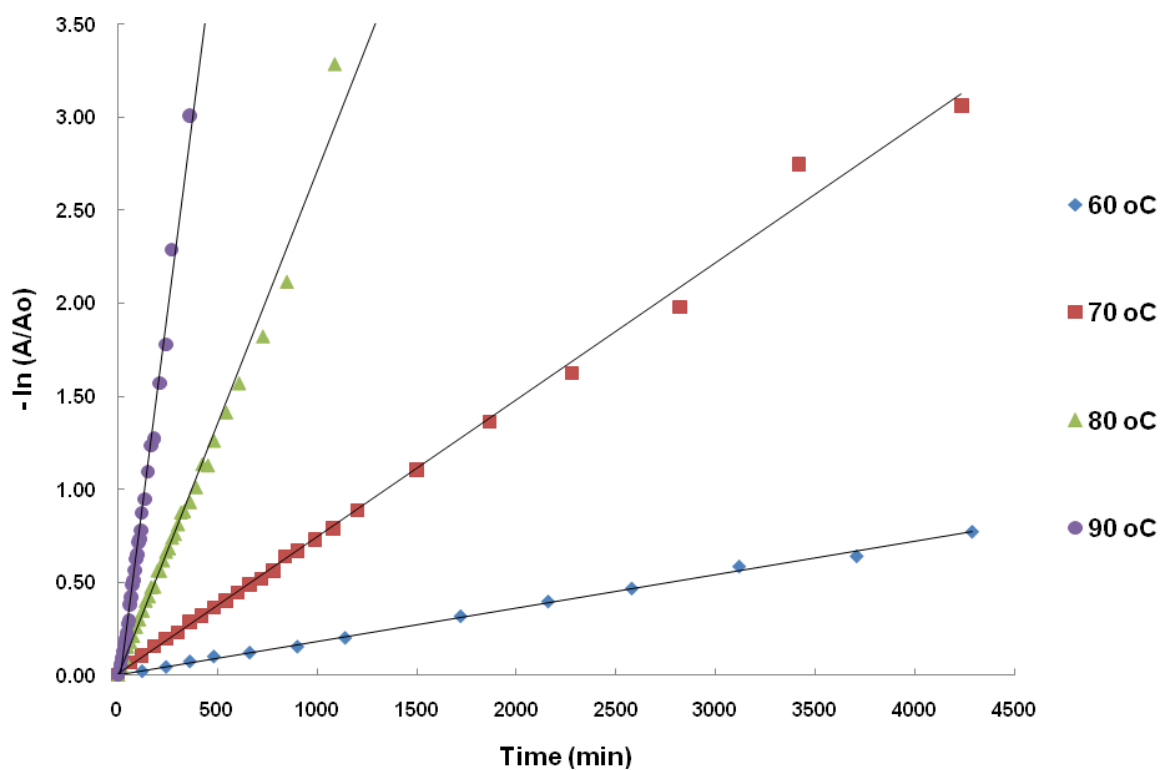


Figure S26. Temperature dependence plot for conversion of **4** to **2-d**₆ in C₆D₆

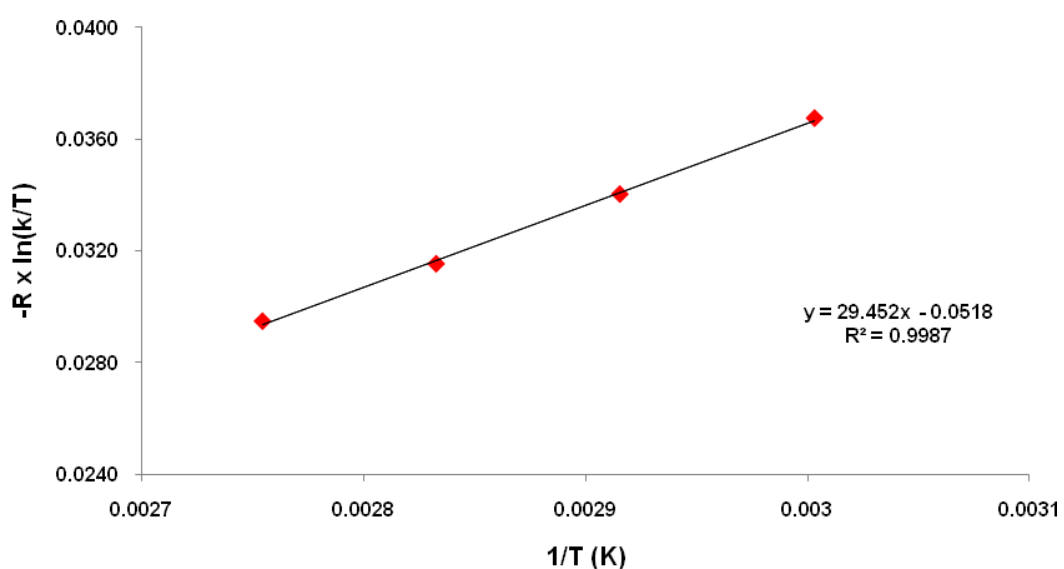


Figure S27. Eyring plot for conversion of **4** to (PNP)Ti=CD^tBu(C₆D₅) (**2-d₆**).

Table S3. Rate constants determined for conversion of **4** to **2-d₆** at different temperatures.

T, °C	60	70	80	90
k, x10 ⁻⁵ s ⁻¹	0.3	1.3	4.3	13.1

Table S3. Rate constants and KIE values determined for thermolysis of **4**, **4-d₁**, **4-d₃** and **4-d₄** in C₆D₆ at 80 °C.

Compound	k (x10 ⁻⁵ s ⁻¹)	KIE
4	4.307	--
4-d₁	2.400	1.79
4-d₃	4.277	1.01
4-d₄	2.094	2.06

Theoretical Section

All calculations were carried out using Density Functional Theory as implemented in the Jaguar 7.0 suite(7) of ab initio quantum chemistry programs. Geometry optimizations were performed with the B3LYP(8-11) functional and the 6-31G** basis set. The transition metals were represented using the Los Alamos LACVP** basis(12-14) that includes relativistic effective core potentials. All geometry optimizations have been carried out in the singlet spin state. The energies of the optimized structures were reevaluated by additional single-point calculations on each optimized geometry using Dunning's correlation-consistent triple- ζ basis set(15) cc-pVTZ(-f) that includes a double set of polarization functions. For all transition metals, we used a modified version of LACVP**, designated as LACV3P**, in which the exponents were decontracted to match the effective core potential with the triple- ζ . Vibrational frequency calculations based on analytical second derivatives at the B3LYP/6-31G** (LACVP**) level of theory were carried out to derive the zero-point-energy (ZPE) and entropy corrections at room temperature utilizing unscaled frequencies. Note that by entropy here we refer specifically to the vibrational/rotational/translational entropy of the solute(s); the entropy of the solvent is implicitly included in the dielectric continuum model.

Solvation energies were evaluated by a self-consistent reaction field (SCRF)(16-19) approach based on accurate numerical solutions of the Poisson-Boltzmann equation. In the results reported, solvation calculations were carried out at the optimized gas-phase geometry employing the dielectric constant of $\epsilon = 2.284$ (benzene). As is the case for all continuum models, the solvation energies are subject to empirical parametrization of the atomic radii that are used to generate the solute surface. We employ the standard set of optimized radii in Jaguar for H (1.150 Å), C (1.900 Å), N (1.600 Å), P (2.074 Å) and Ti (1.587 Å).

The energy components have been computed with the following protocol. The free energy in solution phase $G(\text{Sol})$ has been calculated as follows:

$$G(\text{Sol}) = G(\text{gas}) + G^{\text{solv}} \quad (1)$$

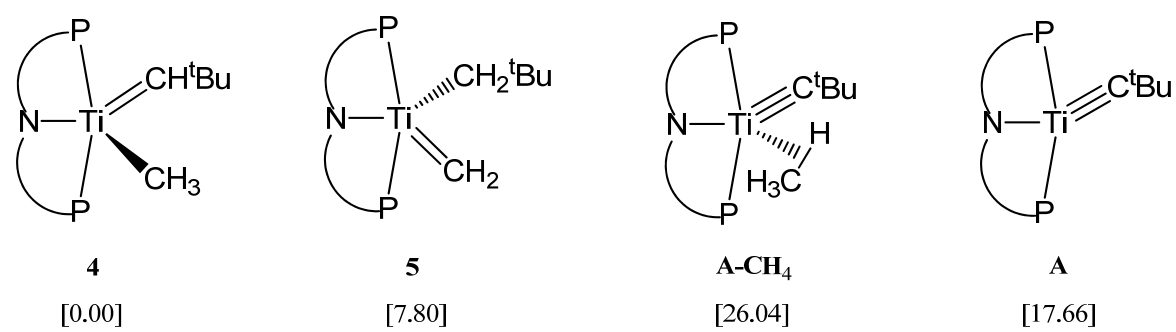
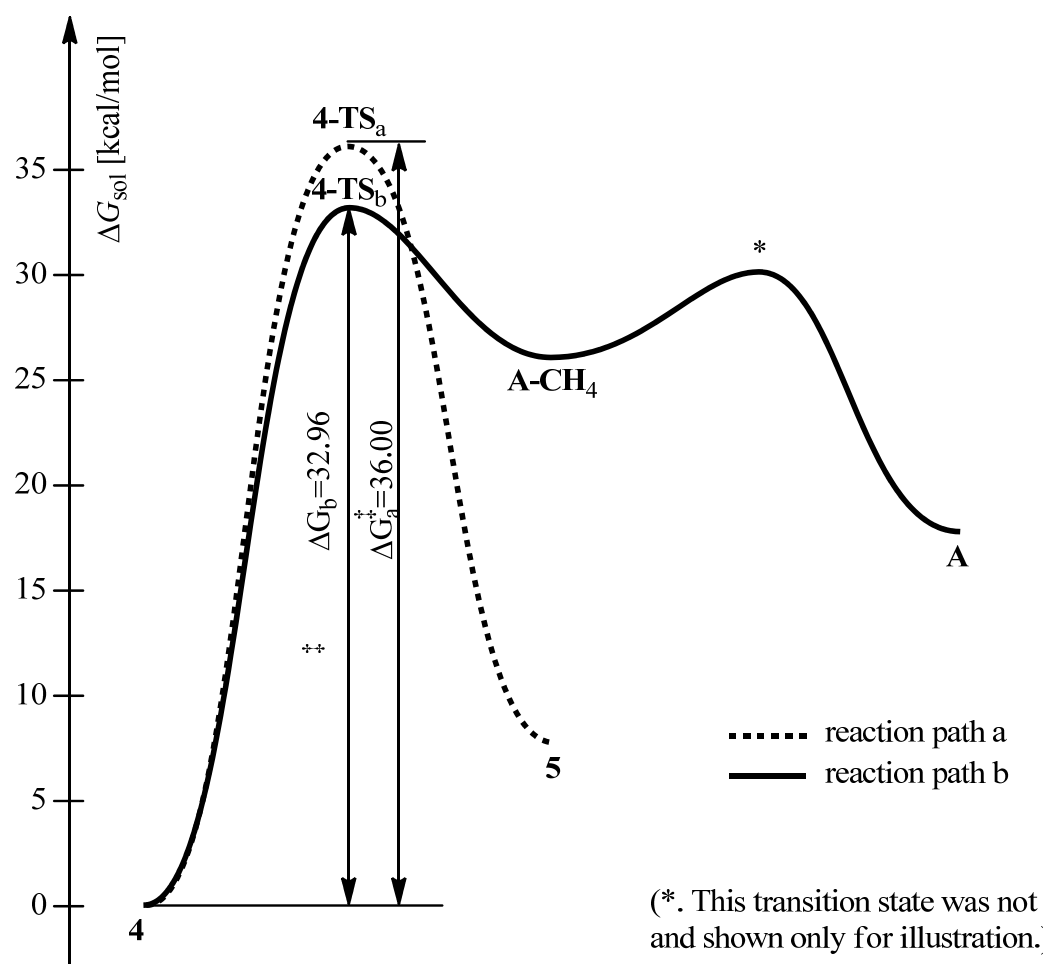
$$G(\text{gas}) = H(\text{gas}) - TS(\text{gas}) \quad (2)$$

$$H(\text{gas}) = E(\text{SCF}) + ZPE \quad (3)$$

$$\Delta E(\text{SCF}) = \sum E(\text{SCF}) \text{ for products} - \sum E(\text{SCF}) \text{ for reactants} \quad (4)$$

$$\Delta G(\text{Sol}) = \sum G(\text{Sol}) \text{ for products} - \sum G(\text{Sol}) \text{ for reactants} \quad (5)$$

$G(\text{gas})$ is the free energy in gas phase; G^{solv} is the free energy of solvation as computed using the continuum solvation model; $H(\text{gas})$ is the enthalpy in gas phase; T is the temperature (298.15K); $S(\text{gas})$ is the entropy in gas phase; $E(\text{SCF})$ is the self-consistent field energy, i.e. “raw” electronic energy as computed from the SCF procedure and ZPE is the zero point energy. Free transition state search was carried out in order to locate transition states, except for the transition state (**4-TS_a**) corresponding to the elimination of methane from **4**, in which case quadratic synchronous transit (QST) search was used.



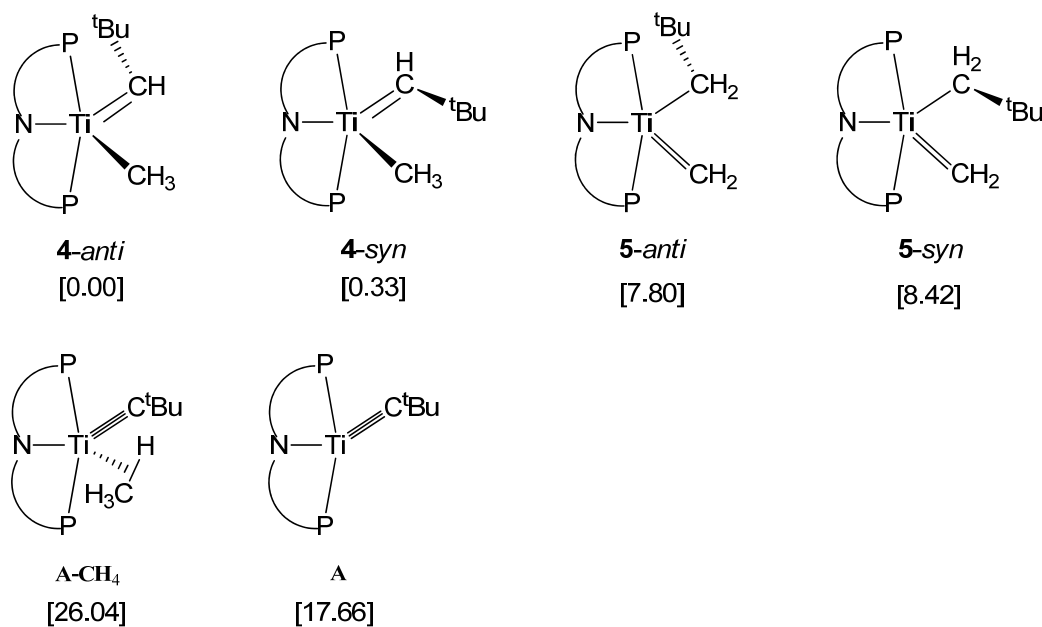


Figure S28. Proposed reaction pathways for methane extrusion (path b) and tautomerization (path a) in complex 4. The alkylidyne precursor and intermediates including alkylidene rotamers, are shown with their respective energies. Values in brackets correspond to computed solution-free energies (ΔG_{sol}) in $\text{kcal}\cdot\text{mol}^{-1}$.

References

- (1) Bailey, B. C.; Huffman, J. C.; Mindiola, D. J.; Weng, W.; Ozerov, O. V. *Organometallics* **2005**, *24*, 1390.
- (2) Bailey, B. C.; Fan, H.; Huffman, J. C.; Baik, M.-H.; Mindiola, D. J. *J. Am. Chem. Soc.* **2005**, *129*, 8781.
- (3) Yousef, R. I.; Walfort, B.; Rueffer, T.; Wagner, C.; Schmidt, H.; Herzog, R.; Steinborn, D. *J. Organomet. Chem.* **2005**, *690*, 1178.
- (4) Owen, J. S.; Labinger, J. A.; Bercaw J. E. *J. Am. Chem. Soc.* **2006**, *128*, 2005.
- (5) Bailey, B. C.; Fout, A. R.; Fan, H.; Tomaszewski, J.; Huffman, J. C.; Mindiola D. J. *Angew. Chem. Int. Ed.* **2007**, *46*, 8246.
- (6) Bailey, B. C.; Fout, A. R.; Fan, H.; Tomaszewski, J.; Huffman, J. C.; Gary, J. B.; Johnson, M. J. A.; Mindiola, D. J. *J. Am. Chem. Soc.* **2007**, *129*, 2234.
- (8) Jaguar 7.0 (Schrödinger, LLC, New York, NY, 2007.).
- (9) Becke, A. D. *J. Chem. Phys.* **1993**, *98*, 5648.

- (10) Vosko, S. H.; Wilk, L.; Nusair M. *Can. J. Phys.* **1980**, *58*, 1200.
- (11) Lee, C. T.; Yang, W. T.; Parr, R. G. *Phys. Rev. B* **1988**, *37*, 785.
- (12) Becke, A. D. *Phys. Rev. A* **1988**, *38*, 3098.
- (13) Wadt, W. R.; Hay, P. J. *J. Chem. Phys.* **1985**, *82*, 284.
- (14) Hay, P. J.; Wadt, W. R. *J. Chem. Phys.* **1985**, *82*, 270.
- (15) Hay, P. J.; Wadt, W. R. *J. Chem. Phys.* **1985**, *82*, 299.
- (16) Dunning, T. H., Jr. *J. Chem. Phys.* **1989**, *90*, 1007.
- (17) Marten, B.; Kyungsun, K.; Cortis, C.; Friesner, R. A.; Murphy, R. B.; Ringnalda, M. N.; Sitkoff, D. Honig, B. *J. Phys. Chem. B* **1996**, *100*, 11775.
- (18) Friedrichs, M.; Zhou, R. H.; Edinger, S. R.; Friesner, R. A. *J. Phys. Chem. B* **1999**, *103*, 3057.
- (19) Edinger, S. R.; Cortis, C.; Shenkin, P. S.; Friesner, R. A. *J. Phys. Chem. B* **1997**, *101*, 1190.